

1



2

3

4

5

6

7

8

9

Peer review status:

10

This is a non-peer-reviewed preprint submitted to EarthArXiv.

11

The manuscript has been submitted to

12

Journal of Cleaner Production

13

14

15

16

17

18

19

20

21

22

23
24
25
26
27
28
29
30
31
32
33
34
35
36
37
38
39
40
41
42
43
44
45
46
47
48
49
50
51
52
53
54
55
56
57

An event-based framework for estimating, tracking, and managing annual methane emissions from upstream oil and gas sites

Mozhou Gao^{1,4}, Zahra Ashena^{1,3}, Steve H.L. Liang^{1,3}, Sina Kiaei^{1,3}, and Sara Saeedi^{1,2}

¹GeoSensorWeb Lab, Department of Geomatics Engineering, Schulich School of Engineering, University of Calgary, 2500 University Dr. NW, Calgary, AB, Canada

²Department of Electrical and Software Engineering, Schulich School of Engineering, University of Calgary, 2500 University Dr. NW, Calgary, AB, Canada

³SensorUp Inc., Calgary, AB, Canada

⁴Kuruktag Emissions Ltd., Coquitlam, BC, Canada

Email: mozhou.gao@ucalgary.ca

Abstract

Accurate reporting of annual site-level methane emissions is increasingly required under emerging regulatory and voluntary frameworks in the oil and gas (O&G) sector. In this study, we present an event-based framework for estimating and tracking annual methane emissions from upstream O&G operations. The framework applies the Emission Event Data Model (EEDM) to spatiotemporally group multi-scale emissions data into discrete events using the concept of Allen's interval algebra and spatial proximity. Following event creation, emissions are categorized into three groups—resolved (known emission rate and duration), partially resolved (known emission rate but unknown duration), and unresolved (unknown emission rate and duration)—to facilitate different management and emissions estimation approaches. Three Monte Carlo-based approaches are developed under the framework. They include (1) estimating durations for partially resolved events using null detection, leak generation, and natural repair processes; (2) estimating emissions from unresolved events based on the minimum detection limit of deployed technologies; and (3) estimating emissions from unresolved events using probabilistic occurrence and best-fit distributions. The methodology enables emissions to be reported and verified at the group level rather than individual observation. To demonstrate estimating emissions using this framework, we created two scenarios and performed emissions estimation using synthetic emission observations based on real emissions data for an upstream O&G site. The proposed framework can be implemented in voluntary initiatives such as Veritas 2.0 and the Oil & Gas Methane Partnership (OGMP) 2.0 and applied as a data management framework for the Measurement, Monitoring, Reporting and Verification (MMRV) framework.

58 **Keywords:** Oil and Gas Methane, Greenhouse Gases, Emissions Data model, Emissions
59 Management, Methane Emissions Reconciliation, Measurement-informed Inventory, MMRV
60 Framework

61

62 **Highlights:** This study addresses the fundamental data integration challenges in emissions
63 estimation and well-suited for aligning with the MMRV framework.

64

65 **1. Introduction**

66 Reducing methane (CH₄) emissions from the oil and gas (O&G) sector is internationally
67 recognized as one of the most cost-effective strategies for mitigating global warming [1]. This
68 effort gained significant momentum following the launch of the Global Methane Pledge [2] at the
69 2021 United Nations Climate Change Conference (COP26), which set an ambitious goal of
70 reducing methane emissions by 30% from 2020 levels by 2030. Since then, stakeholders
71 worldwide have made substantial efforts to develop innovative measurement technologies and
72 emissions estimation frameworks. Regulators, such as the U.S. Environmental Protection Agency
73 (EPA) and the European Commission (EC), have further tightened regulatory requirements in
74 recent years [3,4] to help achieve these reduction targets.

75 The Measuring, Monitoring, Reporting, and Verification (MMRV) framework is widely
76 recognized as one of the most effective frameworks for managing emissions in the oil and gas
77 (O&G) sector and tracking annual emissions [5,6]. Measuring refers to deploying measurement
78 technologies to directly measure and quantify emissions, including remote sensing systems and
79 close-range instruments. For emission sources that have already been identified, monitoring is
80 conducted either through continuous monitoring systems or revisits using snapshot technologies
81 to track emission activity. Reporting refers to standardized documentation and disclosure of
82 emissions data and methodologies applied to calculate emissions to regulatory bodies (e.g., EU)
83 or voluntary programs (e.g., UNEP OGMP 2.0). Verification refers to reviewing and validating
84 reported emissions [5, 6].

85 To date, MMRV is still an ongoing effort, and the equivalent frameworks have primarily been
86 adopted by voluntary initiatives such as the Oil and Gas Methane Partnership (OGMP) 2.0, the
87 MiQ standard, and Veritas 2.0 [7-9]. Some regulatory initiatives, such as Air Quality Control
88 Commission Regulation 7, Part B, implemented by the Colorado Department of Public Health and
89 Environment (CDPHE), have also incorporated similar frameworks [10]. The key objectives of
90 integrating MMRV into emissions reporting and management include guiding the development of
91 measurement technology, establishing an internationally recognized standard to enhance the
92 credibility of emissions reporting, enabling better reconciliation between emissions estimates from
93 bottom-up (BU) and top-down (TD) approaches, creating a measurement-based inventory (MBI)

94 and/or measurement-informed inventory (MII), and assessing overall carbon intensity across the
95 supply chain [5, 6].

96 Various technical challenges and inherent emissions characteristics hinder the effective
97 implementation of MMRV by O&G operators. These challenges include the missing emissions
98 from abnormal events from emissions reporting, the limited availability of measurement data that
99 captures routine operational events, insufficient temporal and spatial coverage of remote O&G
100 sites, undocumented operational activities, inaccuracies in emissions attribution, and the lack of
101 unified measurement scales for emissions data [5,11–13].

102 To address these challenges and generate a more accurate emissions inventory, the scientific
103 community has been actively developing hybrid approaches that integrate both BU and TD data to
104 maximize emissions data utilization, which includes combining measurements results by using
105 multi-scale remote sensing technologies, applying advanced statistical methods, and developing
106 simulation approaches [14–19]. However, a framework and emissions data model to
107 spatiotemporally assimilate emissions data from different measurement scales and estimate
108 emissions that are not measured is still under development. Such a framework can improve
109 emissions management, increase reporting transparency, and enhance uncertainty estimations.

110 This work introduces a novel framework that includes the Emissions Event Data Model (EEDM)
111 designed to spatially and temporally integrate multi-scale emissions measurements with O&G
112 operational data. The model is developed based on the International Organization for
113 Standardization (ISO) 19156:2023 and the Open Geospatial Consortium (OGC) 20-082r4
114 standards, and it integrates with the OGC Sensor Web Enablement suite [20–22]. In the following
115 sections, we will first introduce EEDM and three types of emissions events. Next, we outline the
116 methodology for calculating emissions and uncertainties associated with each type of emission
117 event. Third, we introduce two Monte Carlo approaches for estimating total emissions from
118 unmeasured events (defined as unresolved events in our framework). Finally, we present two case
119 studies to demonstrate our framework using a fictitious site and synthetic emissions data.

120

121 **2. Method and Materials**

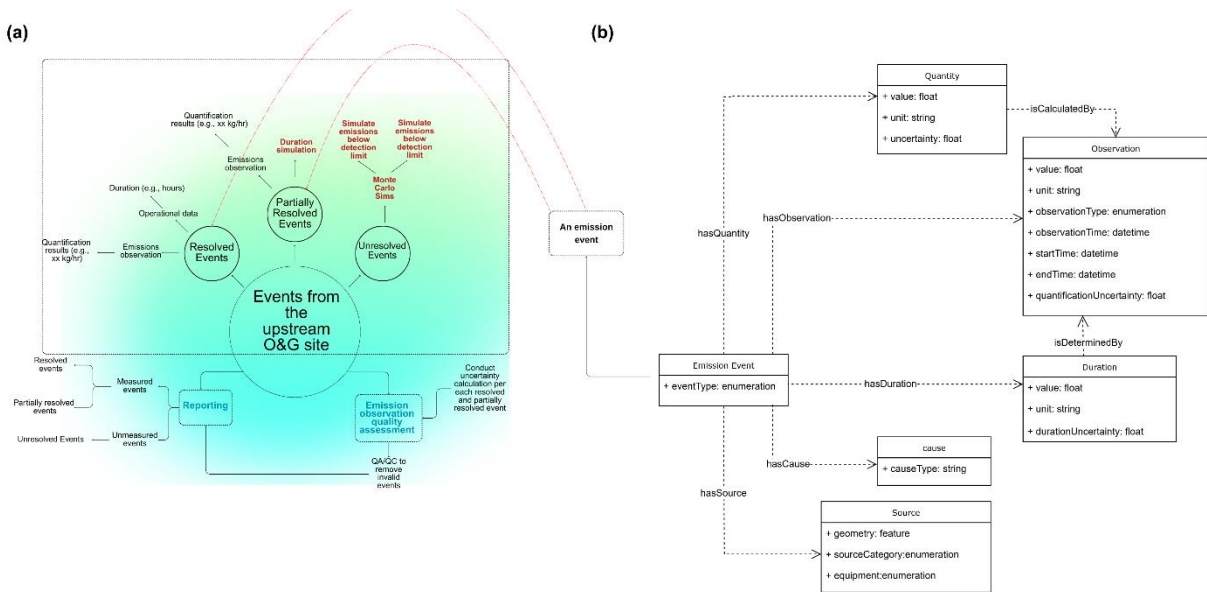
122 2.1 Emissions Event Data Model (EEDM)

123 Conventionally, methane emission data are modeled and managed for each emissions observation
124 (EO). This process captures any form of detection, null-detection, or operational data indicating
125 the presence or absence of CH₄ pollutants in the atmosphere, along with the timing (when) and
126 location (where) of emissions occurred and the quantity (how much) emitted. This information
127 helps attribute each emission observation to a specific physical source (e.g., equipment) and a
128 cause (e.g., fugitive emissions, tank venting, etc.). However, emission observations are typically
129 discrete in time and space, captured at different scales, and quantified using different algorithms.
130 For example, snapshot emission observations, such as aircraft flyover measurements, provide a

131 more accurate quantification of emissions from a site. In contrast, point-based CMS have lower
 132 detection limits and capture emission duration but only measure CH₄ at a fixed location, making
 133 them less accurate than aircraft flyovers in quantifying emissions.

134 To address the challenges, EEDM (Figure 1b) was proposed based on the OGC standards,
 135 including ISO/OGC's Observations and Measurements 19156:2023/OGC 20-082r4 [20] and
 136 W3C/OGC Semantic Sensor Networks [22]. EEDM provides a consistent foundation aimed at
 137 enhancing the estimation of emissions duration and capturing their dynamic aspects, such as the
 138 lifecycle of leaks.

139 As illustrated in Figure 1a, emissions observations (EOs) are grouped into events as part of the
 140 measurement and monitoring process, allowing each event to serve as a container for managing
 141 emissions and their associated sources. Each event is then verified to assess its completeness and
 142 accuracy. Since different types of EO have different characteristics and are constrained by
 143 different factors (for example, satellite measurements are impacted by cloud cover), and different
 144 regulatory or voluntary initiatives may have different quality assurance processes, no specific
 145 QA/QC threshold is set in EEDM. However, EEDM does require the uncertainty of each EO to
 146 be included. For example, the MIQ protocol follows ISO 14044 to evaluate the quality of EOs
 147 [8].



148
 149 **Figure 1. (a) Schematic view of event-based framework; (b) The entities and properties of the**
 150 **EEDM and their relationships. The formal definition can be found in S1 of the Supporting**
 151 **Information (SI).**

152
 153
 154

155 2.2 Spatial and Temporal Correlation of Emissions Event (EE)

156 An emission event (EE) may consist of either a single observation or multiple observations
157 capturing the same emission. To determine whether multiple observations can be grouped in both
158 space and time, we apply spatial proximity [23] and Allen's interval algebra [24]. Spatial proximity
159 assesses whether observations are geographically close or attributed to the same source (e.g.,
160 Compressor No. 1), while Allen's interval algebra (See Table S1) determines the temporal
161 relationships between observations. If two or more observations satisfy any of the other eleven
162 relationships and are also spatially close (or attributed to the same equipment), they are more likely
163 to observe the same emission event.

164 As illustrated in Table S1, thirteen fundamental temporal relationships are defined: *precedes*,
165 *preceded by*, *meets*, *met by*, *overlaps*, *overlapped by*, *contains*, *during*, *starts*, *started by*, *finishes*,
166 *finished by*, and *equals* [24]. Except for *precedes* and *preceded by*, if two or more EOs or EEs
167 satisfy any of the other eleven relationships and are also spatially close (or attributed to the same
168 equipment), they are more likely to originate from the same emission within the same emission
169 event. It is important to highlight that *precedes* and *precededBy* are specifically applied to
170 intermittent emission events that have stopped and started again. In EEDM, we treat intermittent
171 events as separate events.

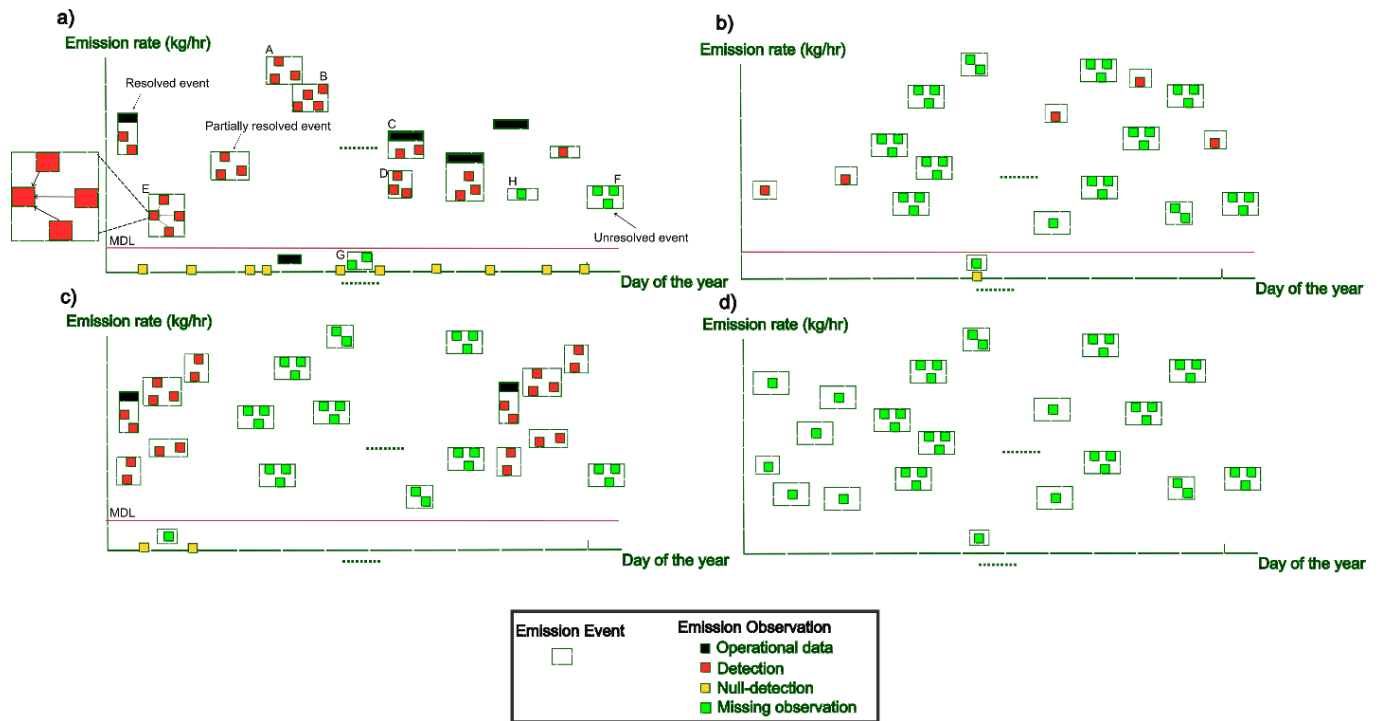
172 In addition to EO, an EE consists of four other primary components: source, cause, duration, and
173 quantity (Figure 1b). The source refers to any equipment or activity that emits methane, and EOs
174 can be attributed to a specific physical source (e.g., Compressor No. 1), a source category (e.g.,
175 fugitive emissions, tank venting), or both (e.g., hydraulic fracturing from a gas well). The cause of
176 an emission event ties to the results of a root cause analysis and is not limited to predefined
177 categories. All observations within the same event should share a common cause. Each observation
178 has its measurement result, associated unit, type of observation (e.g., aircraft flyover - Bridger),
179 observation time that describes when the observation was conducted, start and end time if the
180 observation was reported as a period and quantification uncertainty is quantification is the
181 measurement result.

182 The duration of EE can be either directly measured using CMS (e.g., start and end times) or
183 estimated through indirect observations, such as the absence of emissions or null detection. Both
184 measured and estimated duration have associated uncertainty. Lastly, the quantity represents the
185 total amount of methane emitted during the event. When an event includes multiple measured
186 emissions observations, the observation with the lowest quantification uncertainty is selected to
187 calculate the quantity. When an event includes both calculated and measured emissions, the
188 appropriate quantity should be selected based on the quality, reliability, and relevance of the
189 available data. Some standards, such as Veritas 2.0 [9], guide whether measured or calculated
190 emission results should be used. Such standards can be integrated into the EEDM to determine the
191 quantity for each event. Since quantity is estimated by combining emissions rate quantification
192 and duration estimates, its overall uncertainty reflects the propagation of errors from both sources.

193 The following subsection discusses the mathematical equations used to calculate emission
194 quantities and their associated uncertainties through error propagation.

195

196 2.3 Resolved Event, Partially Resolved Event, and Unresolved Event



197

198 **Figure 2.** Representation of resolved, partially resolved, and unresolved emission events for four
199 sites under different monitoring scenarios throughout the year. The x-axis represents the
200 quantifications of EO associated with each EE. The y-axis represents when emissions are
201 measured and how long they persist in a year. Distinct colors, including operational data,
202 detections, null-detections, and missing observations, indicate various observation types. Green
203 dashed square boxes represent emission events. (a) A site with CMS measuring emissions 24
204 hours a day; (b) A site monitored through flyover surveys conducted every few months; (c) A site
205 with a measurement campaign in which emissions are only measured during the campaign; and
206 (d) A site without any monitoring.

207

208

209

210

211

212

213 **Table 1:** Three categories of emission event types.

| Emission Event Type | Definition | Duration Determination | Emissions Quantity from Events | Uncertainty |
|--------------------------------|--|--|---|--|
| Resolved Event (RE) | Events with durations determined using operational data/log | Extracted from operational data/log | Calculated | Only quantification uncertainty is considered |
| Partially Resolved Event (PRE) | Events with duration that are either measured by remote sensing technologies or estimated using null-detection and rules | Simulated by using proceedings and succeeding null-detection times | Calculated | Quantification uncertainty and duration estimation uncertainty |
| Unresolved Event (UE) | Events that are missing from annual emissions data | Simulated | (1) Simulate emissions that are not detected using POD checks (2) Simulate emissions by random sample RE and PRE | Estimated in the simulations |

214

215 We classify EE into three types (see Table 1): resolved events (REs), partially resolved events
 216 (PREs), and unresolved events (UEs). REs include EOs from data sources such as operational
 217 logs, which can be directly used to estimate duration, attribute sources, and perform root cause
 218 analysis. In contrast, PREs consist solely of EO from measurement technologies. They may
 219 require additional information to determine their duration and root cause, such as estimating
 220 duration using null detections from aircraft flyovers or routine leak detection and repair (LDAR)
 221 surveys that do not identify emissions. The unmeasured and undocumented emissions are
 222 classified as unresolved events (UEs), which can be further classified into three types:

- 223 • **Type 1** occurs when emissions are present, but their rate falls below the deployed
 224 technology's minimum detection limit (MDL) (e.g., event G in Figure 2a). This type of
 225 UE, also known as a false negative, represents an undetected emission event.
- 226 • **Type 2** happens when no measurement technology is deployed to detect the emission
 227 (e.g., event F in Figure 2a).
- 228 • **Type 3** occurs when a small fugitive emission coincides with a large operational event
 229 (e.g., event H in Figure 2a) from the same equipment. Since the emission rates of both
 230 events cannot be separated, Type 3 UEs are typically omitted. Since they are not

231 measured, the reported emissions usually include only the emissions from the large
232 operational event and neglect the small fugitive emissions.

233 Based on the above definitions, we can define the three types of EE mathematically based on the
234 following expressions:

235 Let:

236 E be the set of all emission events.

237 RE , PRE and UE be the subsets of E corresponding to Resolved Events, Partially Resolved
238 Events, and Unresolved Events, respectively.

239 EO_m be the set of emissions observations from measurement technologies.

240 EO_o be the set of emissions observations from operational logs.

241 N be the set of null-detection data (including from screening survey or LDAR inspection).

242 U be the set of emissions data that are not captured by any emissions observations.

243 Then we can define each emission event type as:

244 For resolved events (REs):

$$245 \quad RE = \{e \in E \mid e \text{ has at least one observation from } EO_o\}$$

246 For partially resolved events (PREs):

$$247 \quad PRE = \{e \in E \mid e \text{ has at least one observation from } EO_m \text{ but lacks } EO_o\}$$

248 For unresolved event (UEs):

$$249 \quad UE = \{e \in E \mid e \notin RE \cup PRE\} = \{e \in E \mid e \text{ has no observation from } EO_m \text{ or } EO_o\}$$

250 To ensure that every EE falls into exactly one category:

$$251 \quad E = RE \cup PRE \cup UE,$$

$$252 \quad RE \cup PRE = \emptyset,$$

$$253 \quad RE \cup UE = \emptyset,$$

$$254 \quad PRE \cup UE = \emptyset,$$

255

256 To ensure that each physical emission source (or equipment) has a unique event within each period,
257 we apply spatial proximity and Allen's interval algebra again to merge events. For example, event
258 A and event B can be merged if event A overlaps with event B. Similarly, event C and event D can
259 be merged if event C contains event D, as shown in Figure 1a. After the merging, the duration and

260 quantity are re-calculated. By following the structure of RE, PRE, and UE, annual emissions
261 quantities across all events for a given site (E_{total}) can be calculated as follows:

$$262 \quad E_{Total} = \sum_{i_{RE}=1}^{N_{RE}} E_{RE_i} + \sum_{i_{PRE}=1}^{N_{PRE}} E_{PRE_i} + \sum_{i_{UE}=1}^{N_{UE}} E_{UE_i} \quad Eq.1$$

263 where N_{RE} , N_{PRE} and N_{UE} indicates the number of resolved, partially resolved, and unresolved
264 events, respectively. The E_{RE} , E_{PRE} , and E_{UE} represents total CH₄ emissions quantity from each
265 resolved, partially resolved, and unresolved event, respectively.

266 Based on how measurement technologies are deployed on-site, an upstream O&G site can be
267 measured or monitored under the following scenarios:

- 268 • **Instantaneous screening technology and continuous monitoring systems:** If operational
269 events are reported monthly or yearly, and both instantaneous screening technology and
270 continuous monitoring systems are deployed to the site (Figure 2a), then the annual
271 emissions quantity can be calculated by using all three types of EE.
- 272 • **Instantaneous screening survey only:** If a site has only been surveyed using snapshot
273 measurement technologies, such as bi-monthly flyovers (Figure 2b). In that case, no REs
274 are available and total emissions from E_{RE} is zero, and emissions from REs will be instead
275 simulated as E_{UE} . Thus, annual emissions will be calculated by summing E_{PRE} and E_{UE} .
- 276 • **Measurement campaign only:** If a site has only been surveyed during an annual or bi-
277 annual measurement campaign (Figure 2c) and emissions are also only reported during the
278 measurement campaign, only limited numbers of REs and PREs are measured during the
279 measurement campaign. Thus, E_{UE} to be simulated for periods outside the measurement
280 campaign.
- 281 • **No Emissions data available:** If a site has no measurements at all (Figure 2d), both E_{PRE}
282 and E_{RE} are zero, and E_{UE} needs to be simulated for the entire year.

284 2.4 Generic emissions estimation equation for EE

285 The generic equation of calculating emissions quantity (E) of an event can be described as follows:

$$286 \quad E = Q \times D \quad Eq. 2$$

287 where, Q and D are emission rate, and duration of the event, respectively.

288 2.5 Resolved Event (RE)

289 For REs, the uncertainties associated with each event primarily arise from rate estimation
290 uncertainty. While operational data can be used to estimate event durations, the associated
291 uncertainties are difficult to estimate and are highly variable across different operational practices
292 [25]. Thus, we omit duration uncertainty for REs. However, quantification uncertainty should be
293 accounted for, either by utilizing uncertainty estimates provided by technology vendors or by

294 simulating or calculating it through engineering methods. For example, the quantification
295 uncertainty of the Insight M (was known as Kairos) aircraft system is found to be approximately
296 $\pm 40\%$ [26]. By incorporating the quantification uncertainty ($U_{Q_{RE}}$), the emission estimation of a
297 RE (E_{RE}) can be expressed as follows:

$$298 \quad E_{RE} = Q_{RE} \times D_{opt} \pm U_{Q_{RE}} \times D_{opt} \quad \text{Eq. 3}$$

299 where the emission rate (Q_{RE}) is obtained either from engineering calculations or quantified from
300 measurement technology with the associated emission rate's quantification uncertainty ($U_{Q_{RE}}$).
301 The duration (D_{opt}) is associated with operational data. Therefore, the uncertainty of emissions
302 quantity of RE ($U_{E_{RE}}$) can be calculated by multiplying the quantification uncertainty by the
303 duration. Eq. 3 can also be rewritten as follows:

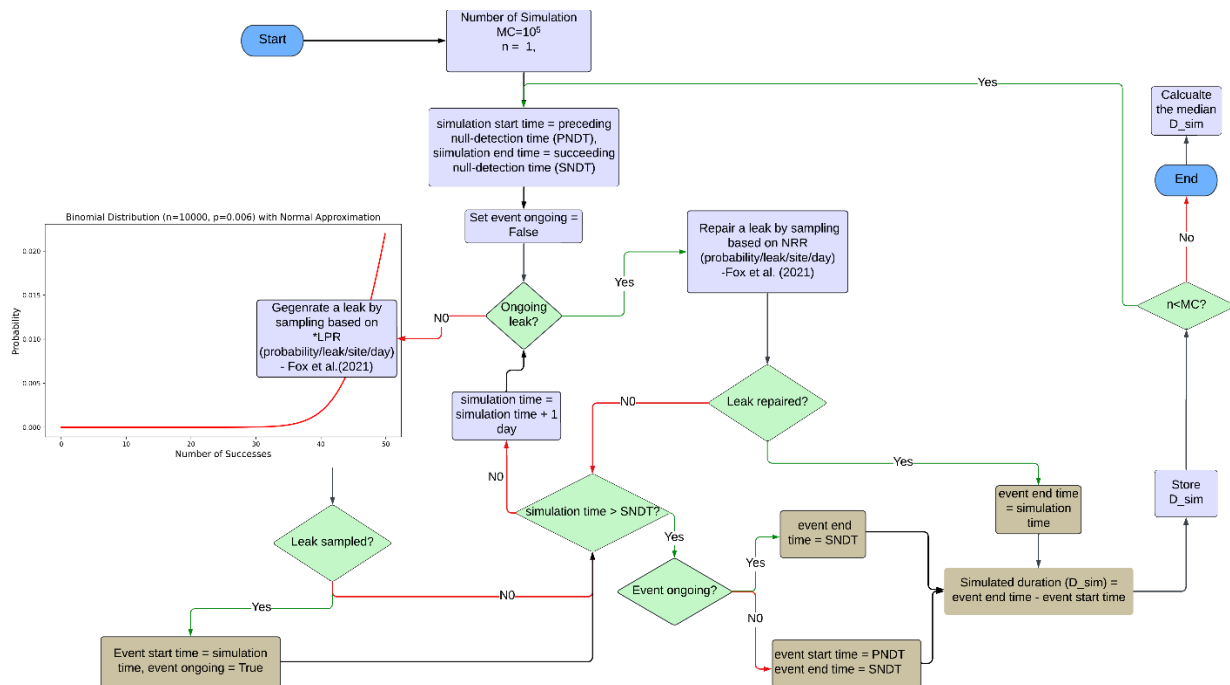
$$304 \quad E_{RE} = Q_{RE} \times D_{opt} \pm U_{E_{RE}} \quad \text{Eq. 4}$$

305 It should be noted that some engineering equations directly calculate emissions quantity. In such
306 cases, the uncertainty should be determined based on the equation used in the calculation.

307 2.6 Partially Resolved Event (PRE)

308 Unlike REs, the uncertainty of PREs must account for both quantification and duration
309 uncertainties. For PREs that include observations from CMS, start and end times are calculated
310 based on measured CH₄ concentrations. However, studies have shown that the resulting durations
311 can significantly differ from actual durations [27, 28]. Addressing this uncertainty requires time
312 series analysis of in-situ wind direction and CH₄ concentration measurements, such as the
313 Probabilistic Duration Model [27]. In contrast, the duration of PREs based solely on instantaneous
314 observations is often estimated using rules or times derived from the preceding null-detects time
315 (PNDT) and succeeding null-detects time (SNDT) [29]. As a result, these duration estimates may
316 either overestimate or underestimate actual durations.

317 To improve duration accuracy for this type of PRE, we developed an event-based Monte Carlo
318 simulation workflow that integrates the leak production rate (LPR) and null repair rate (NRR),
319 both of which are implemented in established stochastic models such as LDAR-Sim and FEAST
320 [30-32].



321

322 **Figure 3.** The Monte Carlo simulation workflow simulates the duration of a PRE based on the
 323 preceding null-detection and succeeding null-detection of the event. In the simulation, the units of
 324 LPR and NRR are per site per day. Here, we present an example binomial distribution with a
 325 probability of 0.006 to sample leaks across 10^5 iterations. *If LPR and NRR are calculated by
 326 equipment or component, the leak sampling and repairing processes iterate through each
 327 equipment or component based on equipment or component counts until all are checked.

328 As shown in Figure 3, a Monte Carlo simulation ($M = 10^5$ iterations) is performed to simulate the
 329 duration to ensure the stationary distribution of results. The start and end times of the simulation
 330 were bounded by the preceding null-detection time (PNDT) and succeeding null-detection time
 331 (SNDT), respectively. Each simulation iteration initializes the emission event as "not occurring."
 332 To determine the start time of the emission event, the simulation randomly samples from a
 333 binomial distribution based on an emission probability calculated using the LPR equation [30]. If
 334 an emission is sampled, the timestamp of the simulation becomes the start time of the emission
 335 event, the simulation updates the status of event as ongoing, and the simulation proceeds to the
 336 next day. Otherwise, the simulation directly proceeds to the next day and repeats the sampling
 337 process. Once an emission event is ongoing, a second binomial distribution, based on a probability
 338 calculated using the NRR equation [30], is used to perform daily random sampling to determine
 339 event cessation. If the event is stopped, the simulation timestamp is saved as the simulated end
 340 time of the event; if not, the process continues to the next day until either the timestamp exceeds
 341 the SNDT, or an end time has been successfully determined. At the end of each simulation run, the
 342 simulated end time is set to the SNDT if the emission event remains ongoing. If no emission event
 343 occurred during the simulation, both the simulated start and end times are set to the PNDT and
 344 SNDT, respectively. The simulated duration is then calculated as the difference between the

345 simulated end and start times. After 10^5 iterations, the mean ($\overline{D_{sim}}$) and 2 times standard deviation
 346 of the differences between simulated and estimated durations are calculated to represent the
 347 uncertainty in duration and the uncertainty from random sampling under the 95% confidence
 348 interval. If simulation results are non-normally distributed, we use median and 2.5- ($D_{sim_{2.5\%}}$)
 349 and 97.5-percentiles ($D_{sim_{97.5\%}}$) to represent simulated duration and uncertainty [33].

350 By integrating both the uncertainty from duration estimation and the uncertainty from
 351 quantification ($U_{E_{PRE}}$), the emissions quantity of each PRE (E_{PRE}) can be calculated by using the
 352 below equation:

$$353 \quad E_{PRE} = Q_{PRE} \times D_{PRE} \pm U_{E_{PRE}} \quad Eq.5$$

354 where the D_{PRE} can be either calculated or simulated:

$$355 \quad D_{PRE} = \begin{cases} T_{end} - T_{start}, & \text{if determined using CMS measurement} \\ \overline{D_{sim}}, & \text{if determined using null detect or rule} \end{cases} \quad Eq.6$$

357 $U_{E_{PRE}}$ represents uncertainties associated with the emissions quantity estimated for each PRE. It
 358 consists of both quantification uncertainty ($U_{Q_{PRE}}$) and duration estimation uncertainty ($U_{D_{PRE}}$),
 359 which can be calculated as follows:

$$360 \quad U_{D_{PRE}} = \begin{cases} PDM(T_{end}, T_{start}, C_{CH4}), & \text{if determined using CMS measurement [27]} \\ [D_{sim_{2.5\%}}, D_{sim_{97.5\%}}], & \text{if determined using nondetect or rule} \end{cases} \quad Eq.7$$

361
 362 To combine both uncertainties from quantification and duration estimations, the error propagation
 363 equations described by IPCC [34] can be used to calculate $U_{E_{PRE}}$:

$$364 \quad U_{E_{PRE}} = \sqrt{(U_{Q_{PRE}})^2 + (U_{D_{PRE}})^2} \quad Eq.8$$

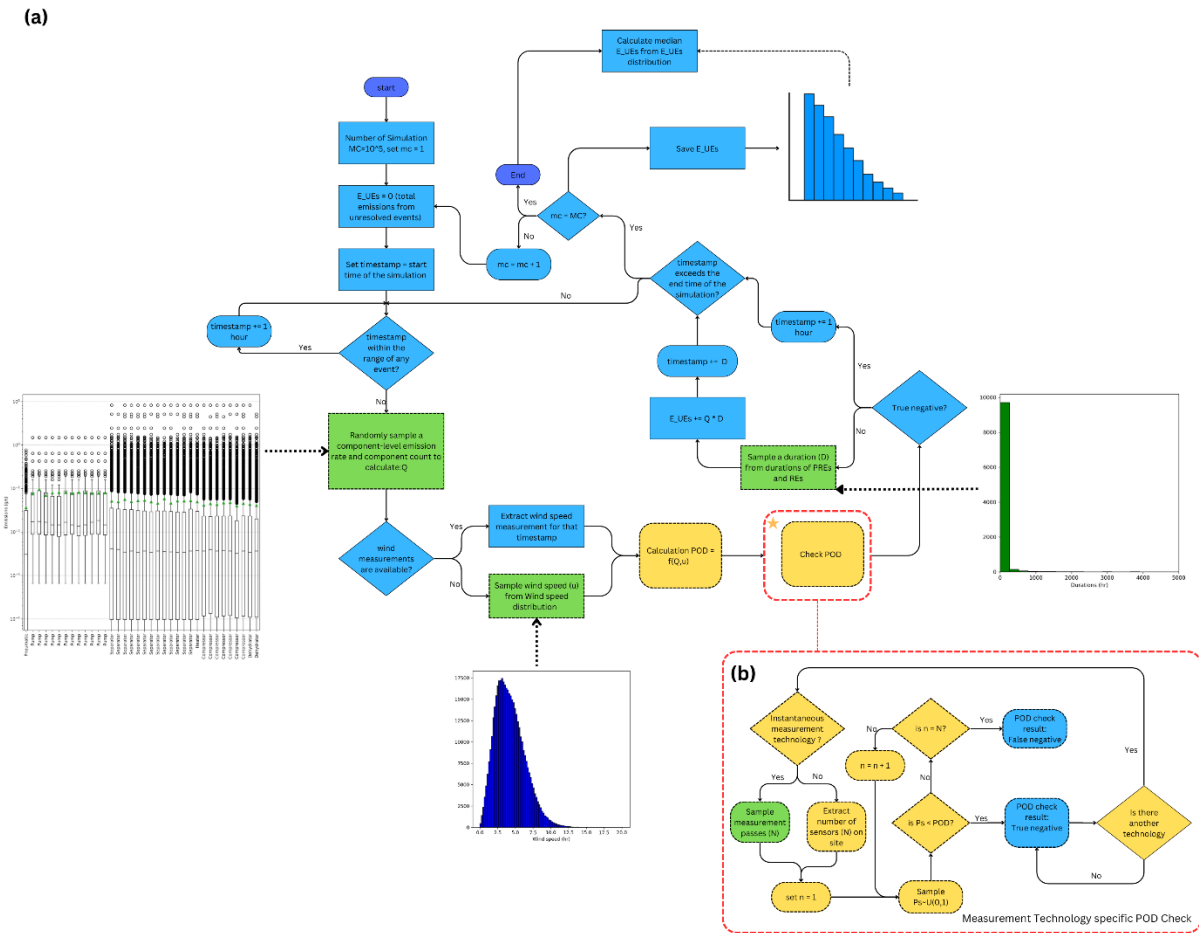
365 The *Eq.8* assumes that duration estimation uncertainty and quantification uncertainty are
 366 uncorrelated. However, this assumption may not always be valid. For instance, in a PRE with a
 367 CMS measurement, the emission rate and duration are both measured by the same sensor,
 368 introducing potential dependencies between the two uncertainties. While this correlation is
 369 important, a detailed investigation is beyond the scope of this study.

370
 371 2.7 Estimating emissions and uncertainty from UEs

372 We developed two distinct simulation approaches to estimate emissions from UEs at a given site.
 373 The first simulation integrates a published methodology [15] into our EEDM framework, using a
 374 probability of detection (POD) equation and a stochastic process to identify UEs below the

375 minimum detection limit (MDL) of the deployed technologies. The second simulation addresses
 376 scenarios in which measurements are insufficient to calculate the annual emissions of a given site
 377 (e.g., the third and fourth scenarios in Figure 2). Instead of relying on POD, it simulates UEs based
 378 on the likelihood of emission event occurrence and precalculated expected emissions rate and
 379 duration distributions.

380 *2.7.1 Simulating Emissions from UEs using probability of detection (POD)*



381
 382 **Figure 4.** Monte Carlo simulation workflow to estimate total emissions from unresolved events
 383 for a given site that is monitored by flyover and CMS. This workflow specifically illustrates the
 384 scenario where emissions are measured by one type of aircraft flyover and one CMS; more
 385 probability of detection (POD) checks are required if other types of technology are also deployed
 386 for emission monitoring. ^aComponent-level emissions distributions should be derived from real
 387 measurements [14]. ^bDifferent aircraft systems require different equations to calculate POD based
 388 on different parameters. For instance, Conrad et al. [35] provided POD equations for three different
 389 aircraft systems. Here, the flowchart only assumes the POD is affected by wind speed. ^cSimilarly,
 390 Bell et al. [28] derived POD equations for multiple CMSs in METEC based on single blind test. It
 391 is also dependent on wind speed. They are applicable in CMS POD checks as well. ^dThe duration

392 distributions are based on empirical data from partially resolved events (PREs) of the site or sites
393 with similar characteristics.

394

395 As illustrated in Figure 4, the simulation workflow begins by initializing the simulation time to the
396 start of the reconciliation period (usually the first day of the year for the annual reconciliation) and
397 setting possible emissions from UEs (E_{UE_sim}) to 0. At each hourly timestep, the simulation checks
398 if the current timestamp falls within the range of any emission event (both RE and PRE). If the
399 timestamp exceeds the simulation range (e.g., the last day of the year), the simulation proceeds to
400 the next iteration. If no emission event occurs in a given timestamp, a component-scale emission
401 rate and component counts are sampled from either the inventory or database containing
402 component-scale measurements to obtain an equipment-scale emission rate. Wind speed and flight
403 passes for each flyover survey at the site location are also randomly sampled.

404 In Figure 4, we are using a site measured by both flyover and CMS as an example. The simulation
405 determines the false negative and identifies if any measurement technology fails to detect an
406 emission independently. Probability of detection (POD)s are calculated using the sampled
407 emission rate and wind speed. Each calculated PODs are then compared to a randomly generated
408 probability (ξ) between 0 and 1. If the POD exceeds ξ , it indicates a false negative (i.e., if the
409 sampled emission occurred in the real world, it would not be detected). If the POD is smaller than
410 ξ , it indicates a true negative (i.e., if the sampled emission occurred in the real world, it would be
411 detected). This comparison is done for each flyover path and each sensor installed on the site. If
412 either the flyover or CMS POD check returns false negative, the sampled emission rate is
413 multiplied by a sampled duration (t_u) to consolidate a UE. Then, the resulted emissions are added
414 to the cumulative E_{UE_sim} . The sampled duration is also added to the time step in the simulation.
415 If POD checks from flyover and CMS both return true negative, meaning no emissions occurred
416 at the time step, the simulation proceeds to the next hour. This process is repeated until the
417 timestamp exceeds the simulation period. Then, the Monte Carlo counter is incremented, and we
418 repeat the whole process until 10^5 iterations are completed. Finally, the mean (\bar{E}_{UE_sim}) and the
419 2.5th and 97.5th percentiles of the E_{UE_sim} distribution are calculated across all simulation
420 iterations to represent the emissions from UEs and their uncertainty.

421

422 *2.7.2 Simulating Emissions from UEs using probability of emission event occurrence*

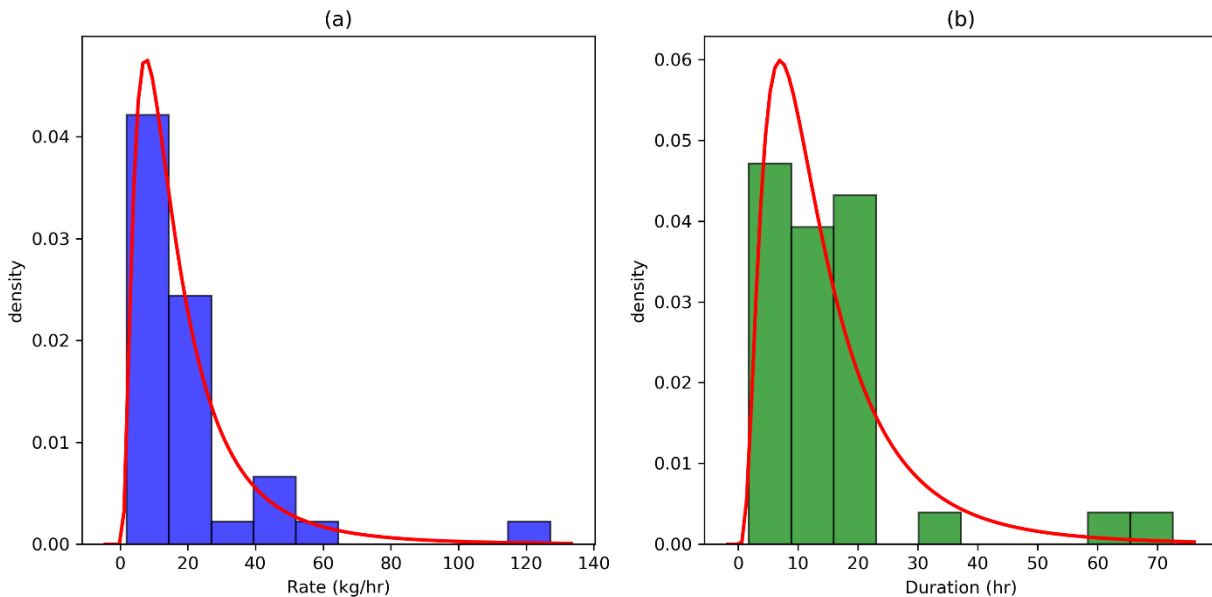
423 A significant limitation in estimating emissions from UEs through the simulation of POD and
424 identifying false negatives is the requirement for extensive temporal coverage of emissions
425 measurements (i.e., either via continuous monitoring systems or frequent instantaneous screening
426 surveys). However, not all sites are monitored sufficiently in the real world. To address this issue,
427 we developed a second simulation approach that simulates UEs based on the probability of
428 emission event occurrence rather than relying on the POD of deployed measurement technologies.

429 Prior to simulation, the following distributions are required to be created from the REs and PREs:

- 430 • The emission rate distribution (Q_{dist}) represents the expected emission rates for a given
431 potential emission source category or equipment.
- 432 • The emission duration distribution (D_{dist}) represents the expected durations for a given
433 potential emission source category or equipment.
- 434 • The probabilities represent the likelihood of an emission event occurrence ($P_{occurrence}$) and
435 not occurrence ($P_{not_occurrence}$) for a given potential emission source category or
436 equipment based on D_{dist} .

437 Since multiple pieces of equipment can emit simultaneously and the emission of one piece is
438 independent of another, sites with more equipment are more likely to have a higher probability of
439 emissions occurring.

440
441 Equipment data and bottom-up inventory are necessary to enhance the simulation results and
442 prevent extrapolating emissions from incorrect source categories. For example, equipment or
443 infrastructure on site can be used to determine the possible emission sources (e.g., emissions from
444 flaring should not be extrapolated for a separator). Similarly, an accurate bottom-up inventory can
445 also be used to constrain the simulation. For example, if liquid unloading never occurred, the
446 simulation should not extrapolate emissions from liquid unloading.



447

448 **Figure 5.** Example of using *Eq.9* to fit empirical rate (a) and duration (b) distributions

449 Since emission rates and durations tend to follow right-skewed distributions, we use a log-normal
450 probability density functions to fit the empirical Q_{dist} and D_{dist} from REs and PREs (e.g., Figure
451 5).

452 $P(v) = ae^{vb}$ Eq.9

453 Where v is the rate or duration sampled under the probability $P(v)$, and a and b are parameters
454 required to fit the rate and duration for each source category or equipment type.

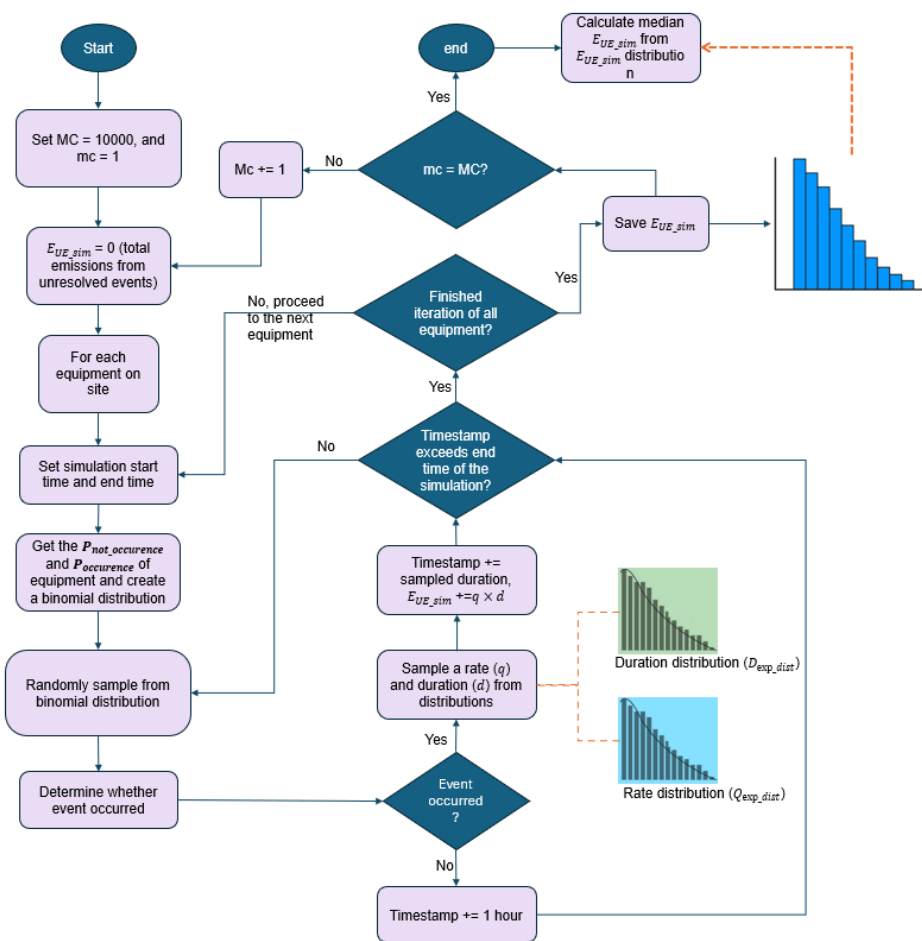
455 After fitting, the log-normal PDF with optimal a and b are used to create the expected rate and
456 duration distributions, Q_{exp_dist} and D_{exp_dist} , for UEs.

457 Unlike creating probability density functions, the combination of an emission event occurrence.
458 Creating binomial distribution [36] based on two probabilities: $P_{occurrence}$ and $P_{not_occurrence}$ can
459 be described as follows:

460
461 $B(x) = \binom{n}{x} P_{occurrence}^x P_{not_occurrence}^{n-x}$ Eq.10

462 Where x is the proportion of time that a source can have an emission event in a given period (n).
463 Since the probability is calculated using duration, $P_{occurrence}$ and $P_{not_occurrence}$, it also describes
464 how frequently a source can have an emission event.

465



466

467 **Figure 6.** A workflow of simulating emissions from UEs by sampling events.

468 Figure 6 describes the workflow of simulations. The Monte Carlo simulation begins by setting the
 469 timestamp to the start time of the simulation and initializing emissions from UEs (E_{UE_sim}) to 0
 470 kg. For each piece of equipment (source category), the simulation proceeds hourly, evaluating the
 471 likelihood of emission occurrence by sampling a binary outcome (0 or 1) based on the
 472 precalculated $P_{occurrence}$ and $P_{not_occurrence}$ of that equipment. If an emission occurs, the emission
 473 rate (q) and duration (d) are sampled from the rate (Q_{exp_dist}) and duration (D_{exp_dist}) distributions,
 474 respectively, to define a UE. The E_{UE_sim} then updated by adding the emissions calculated from
 475 multiplying q and d , and the simulation time is incremented by d . If no emission event occurs, the
 476 simulation time advances by one hour. This process is repeated until the end of the simulation time
 477 for each piece of equipment. The E_{UE_sim} is calculated by summing emissions from all sampled
 478 UEs across all equipment. The simulation is repeated for 10^5 iterations, and the median (\bar{E}_{UE_sim}),
 479 along with the 2.5th and 97.5th percentiles of the E_{UE_sim} distribution, are calculated to represent
 480 the simulated emissions from UEs and their associated uncertainty.

481

482 2.8 Estimating emissions and uncertainties across all EEs

483 By integrating the simulated emissions from UEs (\bar{E}_{UE_sim}), Eq. 4 and Eq. 5 into Eq. 1, it can be
484 rewritten as

$$485 \quad E_{Total} = \sum_{i_{RE}=1}^{N_{RE}} Q_{RE_i} \times D_{opt_i} + \sum_{i_{PRE}=1}^{N_{PRE}} Q_{PRE_i} \times D_{PRE_i} + \bar{E}_{UE_sim} \quad Eq.11$$

486

487 By following the uncertainty equation suggested by IPCC [33], the uncertainties associated with
488 emissions quantity of all REs (U_{E_RES}) and PREs (U_{E_PRE}) can be expressed as follows:

$$489 \quad U_{E_RES} = \frac{\sqrt{(U_{E_RE_1} \times E_{RE_1})^2 + (U_{E_RE_2} \times E_{RE_2})^2 + \dots + (U_{E_RE_{N_{RE}}} \times E_{RE_{N_{RE}}})^2}}{|E_{RE_1} + E_{RE_2} + \dots + E_{RE_{N_{RE}}}|} \quad Eq.12$$

490 and

$$491 \quad U_{E_PREs} = \frac{\sqrt{(U_{E_PRE_1} \times E_{PRE_1})^2 + (U_{E_PRE_2} \times E_{PRE_2})^2 + \dots + (U_{E_PRE_{N_{PRE}}} \times E_{PRE_{N_{PRE}}})^2}}{|E_{PRE_1} + E_{PRE_2} + \dots + E_{PRE_{N_{PRE}}}|} \quad Eq.13$$

492 where U_{E_RE} and U_{E_PRE} are calculated in Eq.3 and Eq.8, respectively.

493 By combining Eq 12-13, the total uncertainty (U_{E_total}) associated with E_{Total} can be calculated
494 as follows:

$$495 \quad U_{E_total} = \frac{\sqrt{(U_{E_RES} \times E_{RES})^2 + (U_{E_PREs} \times E_{PREs})^2 + (U_{E_RES} \times E_{UES})^2}}{|E_{RES} + E_{PREs} + E_{UES}|} \quad Eq.14$$

496

497

498

499

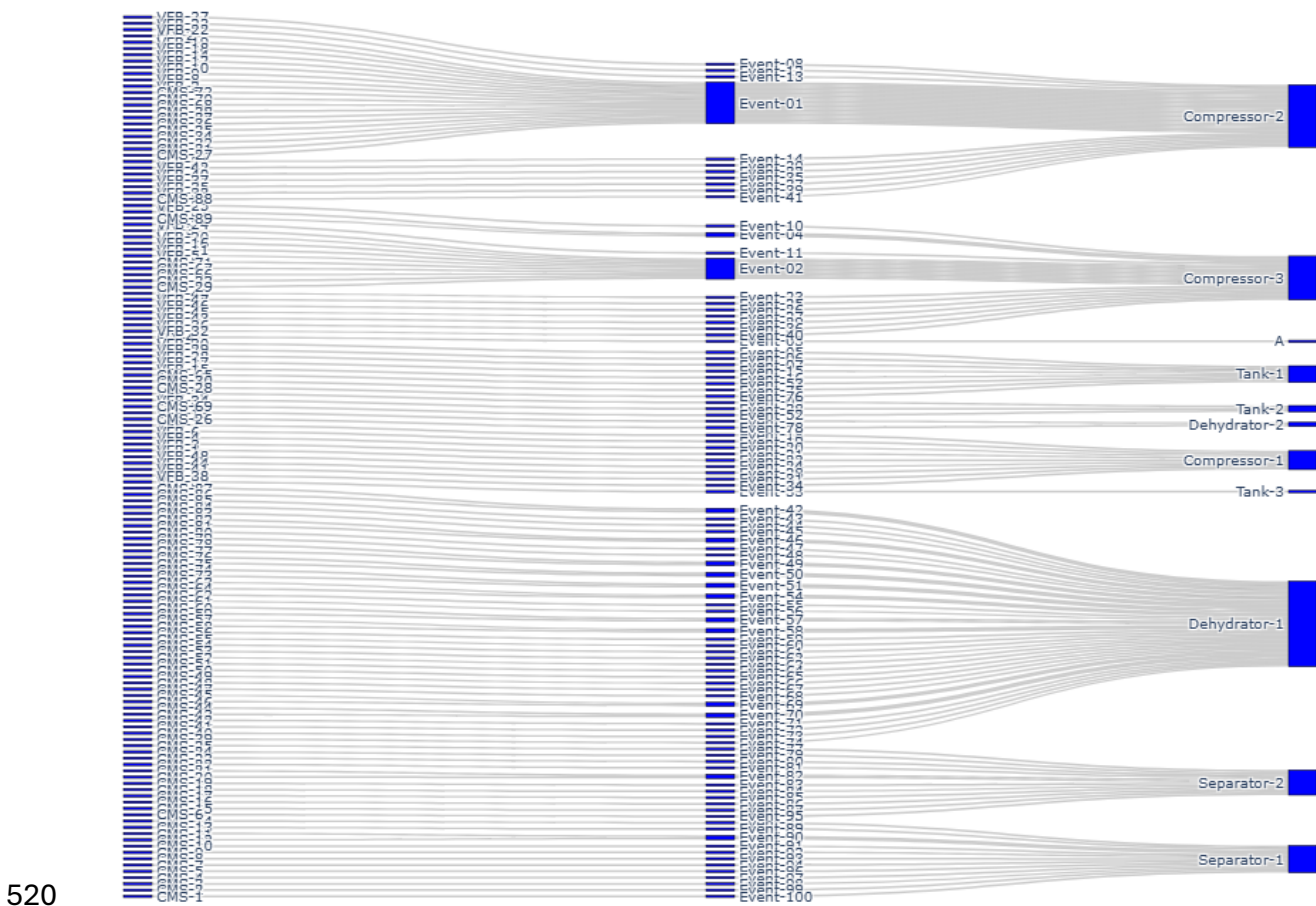
500 **3. Case studies and results**

501 To demonstrate our methodologies, we developed two distinct case studies to estimate total
502 emissions from a fictitious site with ten pieces of equipment from January 1, 2024, to April 30,
503 2024. The first case study utilizes 146 simulated emission observations—including 89 CMS
504 measurements, four flyover survey records (one did not detect any plume), four OGI inspection
505 records (two did not find any leaks), and 49 venting data points. Due to sufficient EOs and all
506 four months being monitored by CMS, we decided to simulate emissions from UEs using a
507 POD-based approach. The second case study extrapolates emissions based on the probability of
508 EE occurrence, using only 36 synthetic CMS observations spanning a single month. In this case,
509 emissions from UEs are simulated based on the probability of an emission event occurring for

510 three unmonitored months. Case Studies 1 and 2 correspond to Scenarios 1 (Figure 2a) and 3
511 (Figure 2c), respectively, as described in Figure 2. All synthetic emission observations can be
512 found in Section S2 of the Supporting Information.

513 These two case studies demonstrate the EEDM's capabilities and provide examples of how
514 annual emissions and their uncertainties can be estimated within the proposed framework.
515 However, real-world applications may require adjustments to the parameters, equations, and
516 simulation logic presented here. For example, it may be necessary to exclude certain months
517 from simulations if sites are shut in during those periods to more accurately reflect operational
518 realities.

519 3.1 Case study No.1



520
521 **Figure 7.** Sankey diagram describing how EOs are merged to EEs and are attributed to
522 equipment in case study No.1.

523 For case study No.1, we initiated 92 PREs and 49 REs. By applying Allen's interval algebra and
524 source attribution results, we merged 41 events, reducing the total number of events to 100,
525 consisting of 61 PREs and 39 REs (Figure 7).

526 To demonstrate the proposed equations, we assume a quantification uncertainty of +/-60% across
527 all events. After merging the events, only one PRE requires duration to be estimated using our
528 proposed duration simulation. The following parameters and assumptions are used to simulate
529 the duration of this PRE: a default LPR of 0.006 leaks/day/site, a 7-day visitation interval, one
530 leak per site at initialization, 10 global leaks, one active leak, and an operator bonus of 0.5. For
531 the remaining PREs, durations were determined based on measured start and end times from
532 CMS observations. Following the findings from Daniels et al. [27], the associated duration
533 uncertainties were assumed to range from 0 to twice the measured durations.

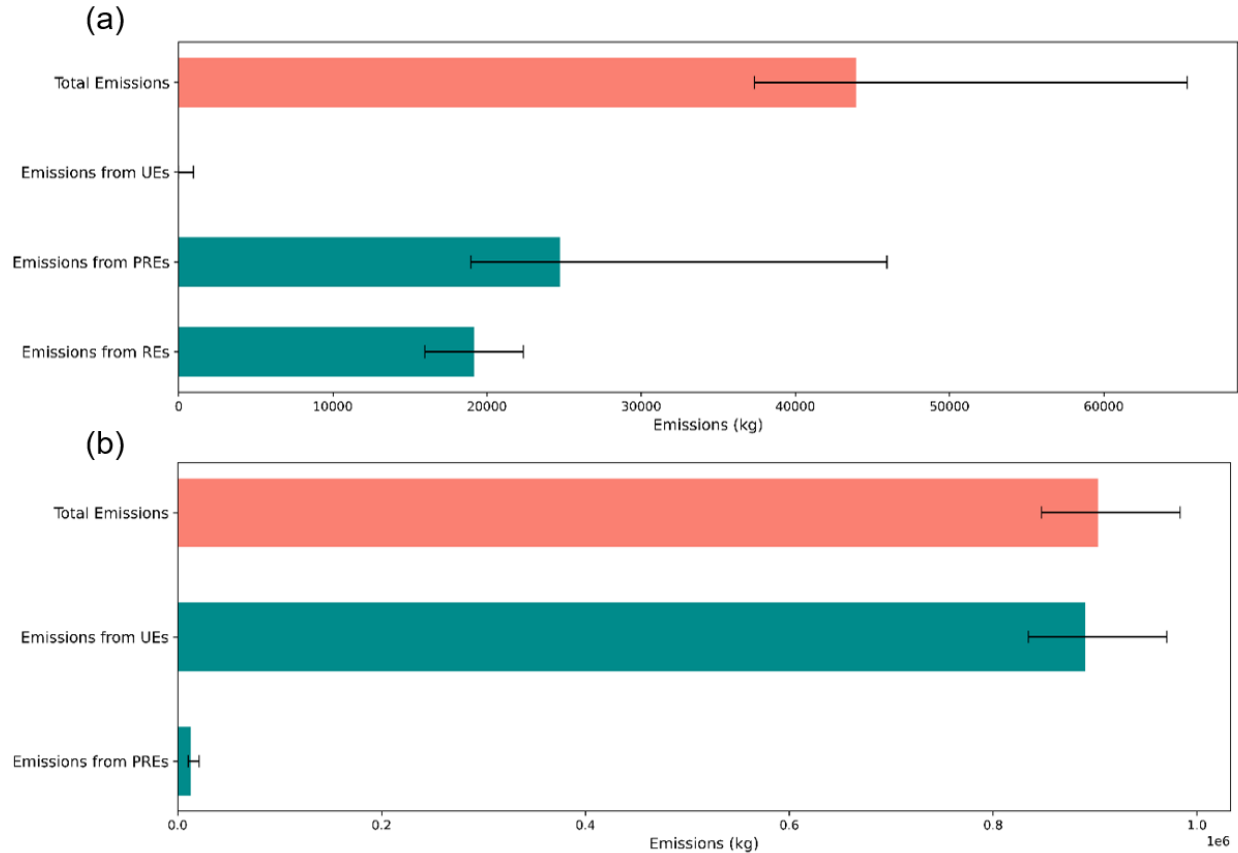
534 The simulation of emissions below the MDL was applied to estimate total emissions from UEs.
535 The following parameters, datasets, and assumptions were used: five CMS sensors were installed
536 on-site; wind speed data from the Permian Basin were obtained from ERA5 [37]; three flight
537 passes were conducted; component-scale emission rates were sampled from empirical
538 component measurements [14]; and POD equations were derived from previous studies [35,38].

539 Figure 8a illustrates the total emissions and their associated uncertainties. After merging the events,
540 only one PRE had its duration estimated using null detections. The resulting distribution of
541 simulated durations was right-skewed, with a median duration of 116.75 hours and a 95%
542 confidence interval (CI) of [4.75, 606.75]. The total emissions over four months are 43922.09 kg,
543 with 95% CI [37336.08, 65408.83]. The breakdown of emissions from REs and PREs are 19167.56
544 kg (95% CI [15959.26, 22375.86]) and 24719.31 kg (95% CI [18967.67, 45945.20]).

545

546 Case studies No.2

547 In the second case study, 36 CMS synthesized observations over a month, initiated 36 PREs.
548 Similar to Case Study 1, we assumed quantification and duration uncertainties of 60% and 200%,
549 respectively, across all PREs. Using Eqs. 9, 10, 14, and 15, the total emissions from PREs were
550 estimated at 12,752.90 kg, with a 95% confidence interval (CI) of [10,318.35, 21,225.40]. After
551 adding 890,185.12 kg of simulated emissions from UEs using the second simulation approach,
552 the total four-month emissions for the fictitious site were 902,938.02 kg, with a 95% CI of
553 [847,296.82, 983,393.09].



554

555 **Figure 8.** The bar chart shows the total site-level emission estimates and breakdown of REs,
 556 PEs, and UEs emissions from (a) case study No.1 and (b) case study No.2.

557

558 **4. Implication & Conclusion**

559 We introduce a new framework integrating multi-scale measurements and O&G operational data
 560 to construct emission events. Adopting ISO and OGC standards ensures that emission events are
 561 compatible across diverse technologies. This integration enhances source attribution and root
 562 cause analysis by combining sensor data with operational records. It highlights the following key
 563 implications:

- 564 • The EEDM represents a simplified data model developed by the ISO 19156 / OGC 20-
 565 082r4 standard and the OGC Sensor Web Enablement suite of standards. It ensures basic
 566 compatibility and interoperability for assimilating sensor data across diverse
 567 measurement technologies. It supports source attribution and cause analysis—two of the
 568 most important follow-up actions for emissions data. A formal data model will be
 569 developed through collaborative group efforts [39].

570

- 571
- 572
- 573
- 574
- 575
- 576
- 577
- 578
- 579
- 580
- 581
- 582
- 583
- 584
- 585
- 586
- 587
- 588
- 589
- 590
- 591
- 592
- 593
- 594
- 595
- 596
- 597
- 598
- 599
- 600
- 601
- 602
- 603
- 604
- 605
- 606
- 607
- 608
- 609
- 610
- Differentiating between REs and PREs improves uncertainty assessments. Past studies have found that most operational events are of short duration [17]. Partitioning emissions from an intermittent source into multiple short-duration events can significantly reduce overall uncertainties associated with its annual emissions estimation, as mathematically, most of the uncertainty in short-duration events stems from quantification rather than both quantification and duration. While measurements from CMSs help reduce duration uncertainty compared to using only snapshot screening technologies, such as aircraft systems, the duration uncertainty associated with CMSs should also be addressed. This is particularly important because surface wind directions often vary on-site, especially at locations with complex infrastructure. Incorporating routine and non-routine operational activity details into the emission event model can further improve the accuracy of duration estimation.
 - We integrated emission events into the methodology developed by Johnson et al. [15], which is sensitive to the PODs of the deployed measurement technologies. Our case studies are based on POD equations derived for InsightM’s aircraft flyovers and Qube’s CMS. If other technologies are simulated, different POD equations should be used, and these should be based on results from controlled release tests.
 - Extrapolation is typically required in two primary scenarios: (1) sites with limited measurements and (2) sites with no events. For sites with limited measurements, accuracy is highly sensitive to the sample size of events (i.e., the number of REs and PREs) used to create the expected rate and duration distributions and calculate probabilities. Both distributions are expected to improve as more events become available for fitting. Future research aims to determine the minimum number of events required to achieve relatively accurate simulation results. Site clustering analysis is often necessary to determine sites with the same characteristics so that CMS data from unmonitored sites can be used to infer emissions from unmonitored sites.
 - In Case Study 2, distributions and probabilities are calculated for each equipment unit. These metrics can also be derived for individual activities or source categories to align with reporting frameworks, such as OGMP 2.0.
 - Beyond site-level emission estimates, EEDM is also suited for responding to the Super-Emitter Program under US EPA regulations [3, 40]. EEDM can more effectively track the source and results from root cause analysis. The start and end times can be more clearly defined by grouping a super-emitter observation (e.g., flyover) and OGI follow-up into a single event.
 - Our model supports the creation of an MII and is compatible with known voluntary initiative frameworks, such as Best-Measured vs. Best-Calculated from Veritas 2.0 and OGMP 2.0 Level 4 and 5 emissions reporting. REs and PREs can be grouped by source to classify events for each source (one class of EEDM). For instance, an MII-based emission factor and its associated uncertainty for flaring can be calculated by dividing the total emissions by the total number of flaring events. To fully align with MMRV, the remaining

611 gap in the framework is the lack of a standard QA/QC process to validate input EOs for
612 emissions quantification and duration estimation. Adding such a standard could ensure that
613 only valid information is included in creating EEs (e.g., using only duration measurements
614 from CMS).

615 This study provides an alternative framework that can be used to estimate annual site-level
616 emissions estimation for the upstream O&G sector. By integrating multiscale emissions
617 observations and operational data using EEDM, annual emissions and associated uncertainties
618 are estimated per each event by combining both quantified rate and estimated durations. The
619 proposed framework has a substantial contribution to ongoing efforts aimed at creating a
620 measurement-informed inventory, improving methane mitigation strategies, and supporting the
621 global objective of reducing methane emissions in the O&G sector. Expanding the scope of our
622 framework to include more types of methane emission data and diverse operational conditions
623 will further enhance its reliability. Adding an event-based QA/QC process could enhance the
624 framework's credibility. Moreover, future studies will also focus on demonstrating this
625 methodology using real-world data across multiple sites to evaluate its feasibility and
626 effectiveness on a broader scale.

627 **Code and Data availability**

628 The analysis was programmed in Python with standard packages. The results can be reproduced
629 by employing the equations, explanations, and parameters provided in the main text. Additional
630 code and data will be made available upon request

631

632 **References**

- 633 1. International Energy Agency. *Global Methane Tracker 2023*; IEA: 2023. Available at:
634 <https://www.iea.org/reports/global-methane-tracker-2023>.
- 635 2. United Nations Framework Convention on Climate Change. *Global Methane Pledge*;
636 UNFCCC: 2021. Available at: <https://www.globalmethanepledge.org>.
- 637 3. U.S. Environmental Protection Agency. *Revisions to GHGRP Subpart W: Petroleum and*
638 *Natural Gas Systems*; U.S. EPA: 2023. Available at: [https://www.epa.gov/inflation-](https://www.epa.gov/inflation-reduction-act/revisions-ghgrp-subpart-w-petroleum-and-natural-gas-systems)
639 [reduction-act/revisions-ghgrp-subpart-w-petroleum-and-natural-gas-systems](https://www.epa.gov/inflation-reduction-act/revisions-ghgrp-subpart-w-petroleum-and-natural-gas-systems).
- 640 4. European Commission. *New EU Methane Regulation to Reduce Harmful Emissions from*
641 *Fossil Fuels in Europe and Abroad*; European Commission: 2024. Available at:
642 [https://energy.ec.europa.eu/news/new-eu-methane-regulation-reduce-harmful-emissions-](https://energy.ec.europa.eu/news/new-eu-methane-regulation-reduce-harmful-emissions-fossil-fuels-europe-and-abroad-2024-05-27_en)
643 [fossil-fuels-europe-and-abroad-2024-05-27_en](https://energy.ec.europa.eu/news/new-eu-methane-regulation-reduce-harmful-emissions-fossil-fuels-europe-and-abroad-2024-05-27_en).
- 644 5. Allen, D.; Ravikumar, A.; Tullos, E. Scientific challenges of monitoring, measuring,
645 reporting, and verifying greenhouse gas emissions from natural gas systems. *ACS*
646 *Sustainable Resour. Manage.* 2023, *1* (1), 10–12.
647 <https://doi.org/10.1021/acssusresmgt.3c00132>.

- 648 6. U.S. Department of Energy. *International MMRV Working Group Reaches Milestone in*
649 *Developing a Credible Framework for Measuring Natural Gas Supply Chain Emissions*;
650 U.S. DOE: 2024. Available at: [https://www.energy.gov/fecm/articles/international-mmrv-](https://www.energy.gov/fecm/articles/international-mmrv-working-group-reaches-milestone-developing-credible-framework)
651 [working-group-reaches-milestone-developing-credible-framework](https://www.energy.gov/fecm/articles/international-mmrv-working-group-reaches-milestone-developing-credible-framework).
- 652 7. United Nations Environment Programme. *The Oil & Gas Methane Partnership 2.0 (OGMP*
653 *2.0)*; UNEP: 2020. Available at: <https://ogmpartnership.com/>.
- 654 8. MiQ. *The MiQ Standard: A Framework for Methane Emissions Assessment*; MiQ: 2024.
655 Available at: <https://miq.org/the-technical-standard/>.
- 656 9. GTI Energy. *Veritas: Ensuring Accurate Methane Emissions Measurements in the Oil and*
657 *Gas Industry*; GTI Energy: 2024. Available at: <https://www.gti.energy/veritas/>.
- 658 10. Colorado Department of Public Health & Environment. *Air Quality Control Commission*
659 *Regulation Number 7*; CDPHE: 2024. Available at: [https://cdphe.colorado.gov/aqcc-](https://cdphe.colorado.gov/aqcc-regulations)
660 [regulations](https://cdphe.colorado.gov/aqcc-regulations).
- 661 11. Vaughn, T. L.; et al. Temporal variability largely explains top-down/bottom-up difference in
662 methane emission estimates from a natural gas production region. *Proc. Natl. Acad. Sci.*
663 *U.S.A.* 2018, *115*, 11712–11717. <https://doi.org/10.1073/pnas.1805687115>.
- 664 12. Brandt, A. R.; Heath, G. A.; Cooley, D. Methane leaks from natural gas systems follow
665 extreme distributions. *Environ. Sci. Technol.* 2016, *50*, 12512–12520.
666 <https://doi.org/10.1021/acs.est.6b04303>.
- 667 13. Scarpelli, T. R.; et al. Updated Global Fuel Exploitation Inventory (GFEI) for methane
668 emissions from the oil, gas, and coal sectors: Evaluation with inversions of atmospheric
669 methane observations. *Atmos. Chem. Phys.* 2022, *22*, 3235–3249.
670 <https://doi.org/10.5194/acp-22-3235-2022>.
- 671 14. Rutherford, J. S.; et al. Closing the methane gap in U.S. oil and natural gas production
672 emissions inventories. *Nat. Commun.* 2021, *12*. <https://doi.org/10.1038/s41467-021-25017-4>.
- 673 15. Johnson, M. R.; Conrad, B. M.; Tyner, D. R. Creating measurement-based oil and gas sector
674 methane inventories using source-resolved aerial surveys. *Commun. Earth Environ.* 2023, *4*.
675 <https://doi.org/10.1038/s43247-023-00769-7>.
- 676 16. Riddick, S. N.; et al. Estimating total methane emissions from the Denver-Julesburg Basin
677 using bottom-up approaches. *Gases* 2024, *4*, 236–252. <https://doi.org/10.3390/gases4030014>.
- 678 17. Wang, J. L.; Daniels, W. S.; Hammerling, D. M.; Harrison, M.; Burmaster, K.; George, F. C.;
679 Ravikumar, A. P. Multiscale methane measurements at oil and gas facilities reveal necessary
680 frameworks for improved emissions accounting. *Environ. Sci. Technol.* 2022, *56*, 14743–
681 14752. <https://doi.org/10.1021/acs.est.2c06211>.
- 682 18. MacKay, K.; et al. A comprehensive integration and synthesis of methane emissions from
683 Canada’s oil and gas value chain. *Environ. Sci. Technol.* 2024, *58*, 14203–14213.
684 <https://doi.org/10.1021/acs.est.4c03651>.
- 685 19. Daniels, W. S.; et al. Toward multiscale measurement-informed methane inventories:
686 Reconciling bottom-up site-level inventories with top-down measurements using continuous
687 monitoring systems. *Environ. Sci. Technol.* 2023, *57*, 11823–11833.
688 <https://doi.org/10.1021/acs.est.3c01121>.
- 689 20. International Organization for Standardization. *ISO 19156:2023 Geographic Information—*
690 *Observations, Measurements, and Samples*; ISO: 2023. Available at:
691 <https://www.iso.org/standard/82463.html#lifecycle>.

- 692 21. Reed, C.; Botts, M.; Percivall, G.; Davidson, J. *OGC® Sensor Web Enablement: Overview*
693 *and High-Level Architecture*; Open Geospatial Consortium: 2013. Available at:
694 <https://docs.ogc.org/wp/07-165r1/>.
- 695 22. World Wide Web Consortium. *Semantic Sensor Network Ontology*; W3C: 2017. Available
696 at: <https://www.w3.org/TR/2017/REC-vocab-ssn-20171019/>.
- 697 23. Anselin, L. Local indicators of spatial association—LISA. *Geogr. Anal.* 1995, 27, 93–115.
698 <https://doi.org/10.1111/j.1538-4632.1995.tb00338.x>.
- 699 24. Allen, J. F. Maintaining knowledge about temporal intervals. *Commun. ACM* 1983, 26, 832–
700 843. <https://doi.org/10.1145/182.358434>.
- 701 25. Higgins, S.; Hecobian, A.; Baasandorj, M.; Pacsi, A. P. A practical framework for oil and gas
702 operators to estimate methane emission duration using operational data. *SPE J.* 2024, 29(5).
703 <https://doi.org/10.2118/219445-pa>.
- 704 26. Sherwin, E. D.; Chen, Y.; Ravikumar, A. P.; Brandt, A. R. Single-blind test of airplane-based
705 hyperspectral methane detection via controlled releases. *Elementa* 2021, 9(1).
706 <https://doi.org/10.1525/elementa.2021.00063>.
- 707 27. Daniels, W. S.; Jia, M.; Hammerling, D. M. Estimating methane emission durations using
708 continuous monitoring systems. *Environ. Sci. Technol. Lett.* 2024, 11, 1187–1192.
709 <https://doi.org/10.1021/acs.estlett.4c00687>.
- 710 28. Bell, C.; et al. Performance of continuous emission monitoring solutions under a single-blind
711 controlled testing protocol. *Environ. Sci. Technol.* 2023, 57, 5794–5805.
712 <https://doi.org/10.1021/acs.est.2c09235>.
- 713 29. Government of Canada. *Regulations Respecting Reduction in the Release of Methane and*
714 *Certain Volatile Organic Compounds (Upstream Oil and Gas Sector) (SOR/2018-66)*;
715 Canada Gazette: 2018. Available at: [https://gazette.gc.ca/rp-pr/p2/2018/2018-04-26/html/sor-
dors66-eng.html](https://gazette.gc.ca/rp-pr/p2/2018/2018-04-26/html/sor-
716 dors66-eng.html).
- 717 30. Fox, T. A.; Gao, M.; Barchyn, T. E.; Jamin, Y. L.; Hugenholtz, C. H. An agent-based model
718 for estimating emissions reduction equivalence among leak detection and repair programs. *J.*
719 *Clean. Prod.* 2021, 282, 125237. <https://doi.org/10.1016/j.jclepro.2020.125237>.
- 720 31. Kemp, C. E.; Ravikumar, A. P.; Brandt, A. R. Comparing natural gas leakage detection
721 technologies using an open-source “Virtual Gas Field” simulator. *Environ. Sci. Technol.*
722 2016, 50, 4546–4553. <https://doi.org/10.1021/acs.est.5b06068>.
- 723 32. Kemp, C. E.; Ravikumar, A. P. *Fugitive Emissions Abatement Simulation Toolkit User*
724 *Guide—FEAST v3.1 Guide & Technical Documentation*; FEAST: 2021. Available at:
725 [https://github.com/FEAST-
SEDLab/FEAST_PtE/blob/FEAST_3.1/FEAST%203.1%20User%20Guide.pdf](https://github.com/FEAST-
726 SEDLab/FEAST_PtE/blob/FEAST_3.1/FEAST%203.1%20User%20Guide.pdf).
- 727 33. Koehler, E.; Brown, E.; Haneuse, S. J.-P. A. On the assessment of Monte Carlo error in
728 simulation-based statistical analyses. *Am. Stat.* 2009, 63(2), 155–162.
729 <https://doi.org/10.1198/tast.2009.0030>.
- 730 34. Intergovernmental Panel on Climate Change. *2006 IPCC Guidelines for National*
731 *Greenhouse Gas Inventories: Volume 1. General Guidance and Reporting*; IGES: 2006.
- 732 35. Conrad, B. M.; Tyner, D. R.; Johnson, M. R. Robust probabilities of detection and
733 quantification uncertainty for aerial methane detection: Examples for three airborne
734 technologies. *Remote Sens. Environ.* 2023, 288, 113499.
735 <https://doi.org/10.1016/j.rse.2023.113499>.
- 736 36. Jowett, G. H. The relationship between the binomial and F distributions. *Statistician* 1963,
737 13(1), 55. <https://doi.org/10.2307/2986663>.

- 738 37. Hersbach, H.; et al. ERA5 hourly data on single levels from 1940 to present. *Copernicus*
739 *Climate Change Service (C3S) Climate Data Store (CDS)* 2023.
740 <https://doi.org/10.24381/cds.adbb2d47>.
- 741 38. MiQ. *Monitoring Technology Compatibility Assessment Qube Axon*; MiQ: 2024. Available
742 at: <https://miq.org/document/qube-compatibility-assessment-2>.
- 743 39. Open Geospatial Consortium. *OGC to Form Emission Event Modeling Language Working*
744 *Group: Public Comment Sought on Charter*; OGC: 2024. Available at:
745 [https://www.ogc.org/requests/ogc-to-form-emission-event-modeling-language-working-](https://www.ogc.org/requests/ogc-to-form-emission-event-modeling-language-working-group-public-comment-sought-on-charter/)
746 [group-public-comment-sought-on-charter/](https://www.ogc.org/requests/ogc-to-form-emission-event-modeling-language-working-group-public-comment-sought-on-charter/).
- 747 40. U.S. Environmental Protection Agency. *Standards of Performance for Crude Oil and*
748 *Natural Gas Facilities for Which Construction, Modification, or Reconstruction Commenced*
749 *after November 15, 2021 (40 C.F.R. § 60 Subpart OOOOb)*; U.S. EPA: 2023. Available at:
750 <https://www.ecfr.gov/current/title-40/chapter-I/subchapter-C/part-60/subpart-OOOOB>.

751

752 **Disclosure statement**

753 No potential conflict of interest was reported by the author (s).

754

755 **Author contributions**

756 M.G and S. L designed the research. M.G. directed and performed the analyses. M.G. and Z. A.
757 wrote the paper. M.G., S.L., Z.A., S.S. and S. K. edited the paper.

758

759

760

761

762

763

764

765

766

767

768

769

770
771
772
773
774
775
776
777
778
779
780
781
782
783
784
785
786
787
788
789
790
791
792
793
794
795
796
797
798

Supporting Information for:

An event-based framework for estimating, tracking, and managing annual methane emissions from upstream oil and gas sites

Mozhou Gao^{1,3,4}, Zahra Ashena^{1,3}, Steve H.L. Liang^{1,3}, Sina Kiaei^{1,3}, and Sara Saeedi^{1,2}

¹GeoSensorWeb Lab, Department of Geomatics Engineering, Schulich School of Engineering, University of Calgary, 2500 University Dr. NW, Calgary, AB, Canada

²Department of Electrical and Software Engineering, Schulich School of Engineering, University of Calgary, 2500 University Dr. NW, Calgary, AB, Canada

³SensorUp Inc, Calgary, AB, Canada

⁴Kuruktag Emissions Ltd, Coquitlam, BC, Canada

Email: mozhou.gao@ucalgary.ca

Table of Contents

S1. Emissions event data model (EEDM) and Allen's time algebra 29

S2. Synthetic emissions observations..... 31

799 S1. Emissions event data model (EEDM) and Allen's time algebra

800 The UML definition of the emissions event data model (EEDM) can be expressed as follows:

```
801     class EmissionsEvent {
802         - eventType: enumeration
803         - hasDuration: Duration
804         - hasCause: Cause
805         - hasSource: Source
806         - hasQuantity: Quantity
807         - hasObservation: Observation[*]
808     }
809
810     class Duration {
811         + value: float
812         + unit: string
813     }
814
815     class Cause {
816         + causeType: string
817     }
818
819     class Source {
820         + geometry: feature
821         + sourceCategory: enumeration
822         + equipment: enumeration
823     }
824
825     class Quantity {
826         + value: float
827         + unit: string
828         - isCalculatedBy: Observation
829         - isDeterminedBy: ObservationF
830     }
831
832     class Observation {
833         + value: float
834         + unit: string
835         + observationType: enumeration
836         + observationTime: datetime
837         + startTime: datetime
838         + endTime: datetime
839     }
840
841     class EventGrouping {
842         - spatialProximity: boolean
843         - temporalRelationship: enumeration
844         - groups: EmissionsEvent[*]
845     }
846
```

847 Where *Observation[*]* in EE allows multiple emissions observations (EOs) to be associated with
848 a single EE. *EventGrouping* class is not included in the Figure 1 of main paper. It represents the
849 logic of grouping EOs using spatial proximity and Allen's interval algebra. The *groups* tracks
850 merged emission events.

851

852 To group EOs into a single EE or merge multiple EEs into one EE, the model uses spatial
 853 proximity to indicate if observations are geographically close or directly/indirectly attributed to
 854 the same physical emission sources (equipment). The *temporalRelationship* indicates the temporal
 855 relations between EOs or EEs based on Allen’s Interval Algebra [1].
 856

857 **Table S1:** Illustration of Allen’s interval algebra logic between two-time intervals.

| Relation | Illustration |
|--------------------|---|
| T1 precedes T2 | T1  |
| T2 precededBy T1 | T2  |
| T1 meets T2 | T1  |
| T2 metBy T1 | T2  |
| T1 overlaps T2 | T1  |
| T2 overlappedBy T1 | T2  |
| T1 starts T2 | T1  |
| T2 startedBy T1 | T2  |
| T1 during T2 | T1  |
| T2 contains T1 | T2  |
| T1 finishes T2 | T1  |
| T2 finishedBy T1 | T2  |
| T1 equals T2 | T1  |

858
 859 As illustrated in Table S1, thirteen fundamental temporal relationships are defined: *precedes*,
 860 *preceded by*, *meets*, *met by*, *overlaps*, *overlapped by*, *contains*, *during*, *starts*, *started by*, *finishes*,
 861 *finished by*, and *equals* [1]. Except for *precedes* and *preceded by*, if two or more EOs or EEs satisfy
 862 any of the other eleven relationships and are also spatially close (or attributed to the same
 863 equipment), they are more likely to originate from the same emission within the same emission
 864 event. For example, we can conclude that the CMS alarm and VFB can be correlated as the same
 865 event, when a CMS alarm indicating emissions from Compressor A between 2024-07-05T09:00:00
 866 and 2024-07-05T11:00:00 *contains* Compressor rod packing venting reported for Compressor A
 867 from 2024-07-05T10:20:00 to 2024-07-05T10:50:00.

868 EEDM uses a network of nodes and edges to identify temporal rules based on relationships
 869 between emission observations within the same event. Each observation is a node within an event,
 870 while edges represent the spatiotemporal correlations between them. The observation with the
 871 earliest timestamp is defined as the parent, and all other observations are considered child
 872 observations. When two events merge, child and parent observations are redefined accordingly.

873 The parent observation plays a crucial role in PREs that contain only instantaneous measurement
 874 observations, particularly when duration must be inferred from preceding and succeeding null
 875 detections.

876 **S2. Synthetic emissions observations**

877 **Table S2.** Synthetic CMS measurements in the case study No.1.

| ID | site | equipment | start time | end time | rate (kg/hr) |
|--------|------|--------------|------------------|------------------|--------------|
| CMS-89 | A | Compressor-3 | 01-01-2024 2:16 | 01-01-2024 18:46 | 13.43743062 |
| CMS-88 | A | Compressor-2 | 01-01-2024 17:12 | 02-01-2024 0:32 | 11.0537834 |
| CMS-87 | A | Dehydrator-1 | 02-01-2024 8:38 | 03-01-2024 2:14 | 6.485984945 |
| CMS-86 | A | Dehydrator-1 | 03-01-2024 1:20 | 03-01-2024 17:55 | 9.745295575 |
| CMS-85 | A | Dehydrator-1 | 03-01-2024 23:33 | 04-01-2024 3:06 | 5.279977194 |
| CMS-84 | A | Dehydrator-1 | 04-01-2024 12:02 | 04-01-2024 20:25 | 44.44340994 |
| CMS-83 | A | Dehydrator-1 | 05-01-2024 12:21 | 05-01-2024 14:09 | 26.4754512 |
| CMS-82 | A | Dehydrator-1 | 05-01-2024 18:40 | 06-01-2024 15:03 | 10.2931667 |
| CMS-81 | A | Dehydrator-1 | 06-01-2024 12:55 | 07-01-2024 6:39 | 22.90488356 |
| CMS-80 | A | Dehydrator-1 | 07-01-2024 3:28 | 07-01-2024 7:34 | 4.38235222 |
| CMS-79 | A | Dehydrator-1 | 07-01-2024 15:50 | 08-01-2024 5:10 | 15.68792648 |
| CMS-78 | A | Dehydrator-1 | 08-01-2024 21:11 | 09-01-2024 5:36 | 23.01335768 |
| CMS-77 | A | Dehydrator-1 | 09-01-2024 4:54 | 09-01-2024 15:33 | 16.46214129 |
| CMS-76 | A | Dehydrator-1 | 09-01-2024 20:05 | 10-01-2024 10:21 | 6.575924082 |
| CMS-75 | A | Dehydrator-1 | 10-01-2024 9:17 | 11-01-2024 20:43 | 9.97428315 |
| CMS-74 | A | Dehydrator-1 | 12-01-2024 8:57 | 15-01-2024 9:31 | 39.60280338 |
| CMS-73 | A | Dehydrator-1 | 15-01-2024 9:19 | 15-01-2024 12:30 | 4.631917288 |
| CMS-72 | A | Compressor-2 | 15-01-2024 11:46 | 16-01-2024 6:06 | 127.1398731 |
| CMS-71 | A | Compressor-3 | 16-01-2024 11:53 | 17-01-2024 3:15 | 50.81348771 |
| CMS-70 | A | Compressor-2 | 17-01-2024 10:29 | 19-01-2024 23:15 | 9.865365612 |
| CMS-69 | A | Tank-2 | 20-01-2024 17:49 | 21-01-2024 0:07 | 7.830741333 |
| CMS-68 | A | Compressor-2 | 21-01-2024 7:16 | 22-01-2024 0:02 | 7.280364451 |
| CMS-67 | A | Compressor-3 | 22-01-2024 2:24 | 22-01-2024 7:15 | 1.872333732 |
| CMS-66 | A | Compressor-3 | 22-01-2024 6:48 | 23-01-2024 1:56 | 11.11957246 |
| CMS-65 | A | Tank-1 | 22-01-2024 13:05 | 23-01-2024 2:59 | 15.78909064 |
| CMS-63 | A | Dehydrator-1 | 23-01-2024 16:02 | 24-01-2024 8:27 | 19.49150927 |
| CMS-64 | A | Dehydrator-1 | 23-01-2024 16:02 | 24-01-2024 6:27 | 27.31177958 |
| CMS-62 | A | Dehydrator-1 | 24-01-2024 15:06 | 25-01-2024 1:46 | 17.92923359 |
| CMS-61 | A | Dehydrator-1 | 25-01-2024 16:45 | 26-01-2024 5:08 | 19.41097409 |
| CMS-60 | A | Dehydrator-1 | 26-01-2024 13:50 | 27-01-2024 6:36 | 22.35054016 |
| CMS-59 | A | Dehydrator-1 | 27-01-2024 1:45 | 27-01-2024 8:08 | 13.98306741 |
| CMS-57 | A | Dehydrator-1 | 27-01-2024 10:10 | 28-01-2024 3:15 | 13.09969511 |
| CMS-58 | A | Dehydrator-1 | 27-01-2024 10:10 | 27-01-2024 23:37 | 16.04159662 |
| CMS-56 | A | Dehydrator-1 | 28-01-2024 15:43 | 28-01-2024 23:59 | 10.05147194 |
| CMS-55 | A | Dehydrator-1 | 29-01-2024 15:48 | 30-01-2024 0:36 | 12.67874941 |

| | | | | | |
|--------|---|--------------|------------------|------------------|-------------|
| CMS-54 | A | Dehydrator-1 | 31-01-2024 17:15 | 01-02-2024 3:30 | 60.47970498 |
| CMS-53 | A | Dehydrator-1 | 01-02-2024 13:45 | 01-02-2024 22:38 | 10.77638599 |
| CMS-52 | A | Dehydrator-1 | 02-02-2024 23:30 | 03-02-2024 6:10 | 24.7853662 |
| CMS-51 | A | Dehydrator-1 | 03-02-2024 11:03 | 03-02-2024 15:53 | 17.19845255 |
| CMS-50 | A | Dehydrator-1 | 04-02-2024 13:38 | 05-02-2024 8:05 | 23.45762222 |
| CMS-49 | A | Dehydrator-1 | 07-02-2024 4:05 | 07-02-2024 9:11 | 14.86192301 |
| CMS-48 | A | Dehydrator-1 | 07-02-2024 17:09 | 07-02-2024 21:40 | 13.72649872 |
| CMS-47 | A | Dehydrator-1 | 08-02-2024 8:39 | 08-02-2024 14:27 | 17.22924512 |
| CMS-45 | A | Dehydrator-1 | 08-02-2024 17:30 | 09-02-2024 4:10 | 11.86600299 |
| CMS-46 | A | Dehydrator-1 | 08-02-2024 17:30 | 09-02-2024 4:10 | 14.76924197 |
| CMS-44 | A | Dehydrator-1 | 10-02-2024 6:47 | 10-02-2024 16:31 | 6.821435342 |
| CMS-43 | A | Dehydrator-1 | 10-02-2024 14:50 | 10-02-2024 23:17 | 28.89126158 |
| CMS-42 | A | Dehydrator-1 | 11-02-2024 15:45 | 12-02-2024 5:38 | 123.3328614 |
| CMS-41 | A | Dehydrator-1 | 16-02-2024 11:51 | 16-02-2024 16:46 | 14.83360889 |
| CMS-40 | A | Dehydrator-1 | 22-02-2024 2:22 | 22-02-2024 9:08 | 17.60689626 |
| CMS-39 | A | Dehydrator-1 | 22-02-2024 11:25 | 23-02-2024 4:36 | 33.41612275 |
| CMS-38 | A | Compressor-2 | 23-02-2024 14:04 | 24-02-2024 3:23 | 18.51180616 |
| CMS-37 | A | Compressor-2 | 24-02-2024 8:34 | 24-02-2024 18:34 | 11.69312178 |
| CMS-36 | A | Compressor-2 | 27-02-2024 10:58 | 27-02-2024 15:44 | 14.44655555 |
| CMS-35 | A | Compressor-2 | 01-03-2024 17:52 | 01-03-2024 23:27 | 16.77220239 |
| CMS-34 | A | Compressor-2 | 03-03-2024 4:38 | 03-03-2024 22:15 | 17.15981442 |
| CMS-33 | A | Compressor-3 | 07-03-2024 5:57 | 07-03-2024 10:56 | 11.42898031 |
| CMS-32 | A | Compressor-2 | 07-03-2024 7:16 | 07-03-2024 15:02 | 16.23481555 |
| CMS-31 | A | Compressor-2 | 08-03-2024 12:23 | 10-03-2024 0:18 | 14.71608663 |
| CMS-29 | A | Compressor-3 | 14-03-2024 9:15 | 14-03-2024 23:52 | 15.29498708 |
| CMS-30 | A | Tank-1 | 14-03-2024 9:15 | 14-03-2024 23:52 | 14.74954203 |
| CMS-28 | A | Tank-1 | 15-03-2024 7:54 | 15-03-2024 19:43 | 10.83058592 |
| CMS-27 | A | Compressor-2 | 18-03-2024 15:35 | 19-03-2024 1:32 | 13.08735161 |
| CMS-25 | A | Separator-2 | 21-03-2024 16:45 | 22-03-2024 2:54 | 12.4923744 |
| CMS-26 | A | Dehydrator-2 | 21-03-2024 16:45 | 22-03-2024 2:54 | 15.49997366 |
| CMS-24 | A | Separator-2 | 22-03-2024 11:45 | 23-03-2024 4:40 | 19.45596602 |
| CMS-23 | A | Separator-2 | 23-03-2024 15:56 | 24-03-2024 8:16 | 20.77621499 |
| CMS-22 | A | Separator-2 | 29-03-2024 12:10 | 29-03-2024 18:10 | 50.5477992 |
| CMS-21 | A | Separator-2 | 05-04-2024 14:08 | 05-04-2024 17:58 | 19.2303107 |
| CMS-20 | A | Separator-2 | 05-04-2024 15:40 | 05-04-2024 20:41 | 53.27457756 |
| CMS-19 | A | Separator-2 | 06-04-2024 1:59 | 06-04-2024 5:50 | 18.95548269 |
| CMS-18 | A | Separator-2 | 09-04-2024 8:27 | 09-04-2024 19:36 | 18.53332709 |
| CMS-17 | A | Separator-2 | 10-04-2024 14:25 | 11-04-2024 0:11 | 140.6241274 |
| CMS-16 | A | Separator-2 | 11-04-2024 15:06 | 11-04-2024 22:43 | 55.89072104 |
| CMS-15 | A | Separator-2 | 12-04-2024 14:09 | 12-04-2024 22:15 | 29.79022037 |
| CMS-14 | A | Separator-1 | 13-04-2024 0:00 | 13-04-2024 8:05 | 14.72482916 |
| CMS-13 | A | Separator-1 | 14-04-2024 1:54 | 14-04-2024 5:54 | 16.01493411 |
| CMS-11 | A | Separator-1 | 16-04-2024 4:25 | 16-04-2024 10:40 | 13.04163146 |

| | | | | | |
|--------|---|-------------|------------------|------------------|-------------|
| CMS-12 | A | Separator-1 | 16-04-2024 4:25 | 16-04-2024 10:40 | 9.677583744 |
| CMS-10 | A | Separator-1 | 17-04-2024 5:04 | 17-04-2024 14:09 | 24.53500301 |
| CMS-9 | A | Separator-1 | 18-04-2024 13:26 | 18-04-2024 20:51 | 14.93944563 |
| CMS-8 | A | Separator-1 | 18-04-2024 22:32 | 19-04-2024 2:41 | 17.65106764 |
| CMS-7 | A | Separator-1 | 19-04-2024 14:49 | 20-04-2024 2:49 | 35.81272269 |
| CMS-6 | A | Separator-2 | 20-04-2024 14:10 | 20-04-2024 16:35 | 77.00366334 |
| CMS-5 | A | Separator-1 | 22-04-2024 14:00 | 23-04-2024 10:07 | 77.63196097 |
| CMS-4 | A | Separator-1 | 26-04-2024 10:15 | 26-04-2024 16:38 | 10.80466042 |
| CMS-3 | A | Separator-1 | 27-04-2024 6:05 | 27-04-2024 13:57 | 16.03540446 |
| CMS-2 | A | Separator-1 | 28-04-2024 7:12 | 28-04-2024 19:16 | 11.16171355 |
| CMS-1 | A | Separator-1 | 29-04-2024 23:25 | 30-04-2024 4:48 | 29.86309642 |

878

879 **Table S3.** Synthetic flyover measurements in the case study No.1.

| ID | site | equipment | detection time | detection | survey time | rate (kg/hr) |
|-------|------|--------------|------------------|-----------|------------------|--------------|
| FLY-1 | A | | | FALSE | 07-01-2024 17:31 | 1538.3 |
| FLY-2 | A | Compressor-2 | 22-02-2024 19:40 | TRUE | 22-02-2024 15:40 | 53 |
| FLY-3 | A | Compressor-3 | 22-03-2024 19:40 | TRUE | 22-03-2024 16:40 | 64 |
| FLY-4 | A | | 05-04-2024 19:14 | TRUE | 05-04-2024 16:14 | 38.5 |

880

881 **Table S4.** Synthetic OGI measurements in the case study No.1.

| ID | site | equipment | detection | survey time | number of leaks |
|-------|------|--------------|-----------|------------------|-----------------|
| OGI-1 | A | | FALSE | 01-01-2024 17:31 | 0 |
| OGI-2 | A | Compressor-2 | TRUE | 01-02-2024 15:40 | 2 |
| OGI-3 | A | Separator-2 | TRUE | 01-03-2024 16:40 | 4 |
| OGI-4 | A | | FALSE | 01-04-2024 16:14 | 0 |

882

883 **Table S5.** Synthetic venting events in the case study No.1.

| ID | site | equipment | start time | end time | total emissions (kg) |
|-------|------|--------------|------------------|------------------|----------------------|
| OP-1 | A | Compressor-3 | 01-01-2024 4:25 | 01-01-2024 4:35 | 182.79626 |
| OP-2 | A | Tank-1 | 01-01-2024 13:34 | 01-01-2024 13:40 | 231.25869 |
| OP-3 | A | Tank-1 | 02-01-2024 6:50 | 02-01-2024 6:57 | 159.22217 |
| OP-4 | A | Tank-1 | 03-01-2024 15:15 | 03-01-2024 15:20 | 263.07187 |
| OP-5 | A | Compressor-2 | 05-01-2024 7:30 | 05-01-2024 7:35 | 339.0873 |
| OP-6 | A | Tank-2 | 06-01-2024 0:40 | 06-01-2024 0:50 | 263.41729 |
| OP-7 | A | Compressor-3 | 06-01-2024 11:30 | 06-01-2024 11:35 | 263.41729 |
| OP-8 | A | Compressor-3 | 06-01-2024 17:25 | 06-01-2024 17:30 | 333.67572 |
| OP-9 | A | Compressor-2 | 07-01-2024 1:30 | 07-01-2024 1:35 | 537.58866 |
| OP-10 | A | Compressor-2 | 07-01-2024 9:30 | 07-01-2024 9:35 | 3515.5696 |
| OP-11 | A | Compressor-2 | 07-01-2024 11:00 | 07-01-2024 11:05 | 335.88641 |

| | | | | | |
|-------|---|--------------|------------------|------------------|-----------|
| OP-12 | A | Compressor-3 | 08-01-2024 9:35 | 08-01-2024 9:40 | 311.91426 |
| OP-13 | A | Compressor-2 | 10-01-2024 7:30 | 10-01-2024 7:35 | 390.3246 |
| OP-14 | A | Compressor-2 | 10-01-2024 9:50 | 10-01-2024 9:55 | 401.44712 |
| OP-15 | A | Tank-1 | 12-01-2024 9:45 | 12-01-2024 10:35 | 606.50225 |
| OP-16 | A | Compressor-3 | 23-01-2024 7:10 | 23-01-2024 7:15 | 416.32321 |
| OP-17 | A | Tank-1 | 25-01-2024 9:00 | 25-01-2024 10:00 | 432.74218 |
| OP-18 | A | Compressor-2 | 03-02-2024 7:40 | 03-02-2024 7:45 | 339.84722 |
| OP-19 | A | Dehydrator-2 | 05-02-2024 14:14 | 16-02-2024 11:45 | 2.0650047 |
| OP-20 | A | Compressor-2 | 10-02-2024 8:41 | 10-02-2024 8:45 | 307.9995 |
| OP-21 | A | Compressor-3 | 10-02-2024 9:04 | 10-02-2024 9:07 | 480.05704 |
| OP-22 | A | Compressor-2 | 10-02-2024 10:14 | 10-02-2024 10:16 | 541.158 |
| OP-23 | A | Compressor-2 | 10-02-2024 11:00 | 10-02-2024 11:03 | 423.1395 |
| OP-24 | A | Compressor-2 | 13-02-2024 8:30 | 13-02-2024 9:10 | 382.33676 |
| OP-25 | A | Compressor-1 | 25-02-2024 7:22 | 25-02-2024 7:24 | 413.12232 |
| OP-26 | A | Compressor-1 | 26-02-2024 14:35 | 26-02-2024 14:37 | 615.999 |
| OP-27 | A | Compressor-3 | 29-02-2024 17:20 | 29-02-2024 17:25 | 309.03576 |
| OP-28 | A | Compressor-1 | 01-03-2024 11:45 | 01-03-2024 11:50 | 278.43155 |
| OP-29 | A | Compressor-1 | 16-03-2024 11:10 | 16-03-2024 11:15 | 347.5616 |
| OP-30 | A | Compressor-2 | 18-03-2024 9:10 | 18-03-2024 9:15 | 212.77872 |
| OP-31 | A | Compressor-1 | 20-03-2024 14:45 | 20-03-2024 14:47 | 513.98496 |
| OP-32 | A | Compressor-3 | 02-04-2024 10:23 | 02-04-2024 10:26 | 454.11216 |
| OP-33 | A | Compressor-1 | 06-04-2024 9:20 | 06-04-2024 9:26 | 245.70876 |
| OP-34 | A | Compressor-3 | 20-04-2024 13:19 | 20-04-2024 13:24 | 288.05024 |
| OP-35 | A | Compressor-3 | 22-04-2024 3:03 | 22-04-2024 3:14 | 123.09513 |
| OP-36 | A | Compressor-3 | 22-04-2024 6:40 | 22-04-2024 6:45 | 320.91821 |
| OP-37 | A | Compressor-1 | 23-04-2024 8:20 | 23-04-2024 8:25 | 415.77054 |
| OP-38 | A | Compressor-3 | 23-04-2024 11:40 | 23-04-2024 11:45 | 385.90322 |
| OP-39 | A | Compressor-2 | 26-04-2024 0:12 | 26-04-2024 0:35 | 53.88552 |
| OP-40 | A | Compressor-1 | 26-04-2024 22:20 | 26-04-2024 22:30 | 119.37715 |
| OP-41 | A | Compressor-2 | 27-04-2024 8:24 | 27-04-2024 8:35 | 147.85023 |
| OP-42 | A | Tank-3 | 27-04-2024 15:08 | 27-04-2024 15:24 | 122.45859 |
| OP-43 | A | Compressor-1 | 29-04-2024 23:13 | 29-04-2024 23:20 | 176.32869 |
| OP-44 | A | Compressor-2 | 29-04-2024 23:20 | 29-04-2024 23:26 | 229.5124 |
| OP-45 | A | Compressor-3 | 30-04-2024 2:05 | 30-04-2024 2:13 | 266.69303 |
| OP-46 | A | Compressor-2 | 30-04-2024 4:10 | 30-04-2024 4:19 | 221.6445 |
| OP-47 | A | Tank-2 | 30-04-2024 6:37 | 30-04-2024 6:50 | 1152.1794 |
| OP-48 | A | Compressor-2 | 30-04-2024 8:12 | 30-04-2024 8:23 | 109.69702 |
| OP-49 | A | Compressor-3 | 30-04-2024 9:50 | 30-04-2024 9:58 | 182.61204 |

884

885

886

887

888 **Table S6.** Synthetic CMS measurement in the case study No.2.

| ID | site | equipment | start time | end time | rate (kg/hr) |
|--------|------|--------------|------------------|------------------|--------------|
| CMS-1 | B | Compressor-3 | 01-01-2024 2:16 | 01-01-2024 18:46 | 13.43743062 |
| CMS-2 | B | Compressor-2 | 01-01-2024 17:12 | 02-01-2024 0:32 | 11.0537834 |
| CMS-3 | B | Tank-1 | 02-01-2024 8:38 | 03-01-2024 2:14 | 6.485984945 |
| CMS-4 | B | Dehydrator-1 | 03-01-2024 1:20 | 03-01-2024 17:55 | 9.745295575 |
| CMS-5 | B | Tank-1 | 03-01-2024 23:33 | 04-01-2024 3:06 | 5.279977194 |
| CMS-6 | B | Separator-1 | 04-01-2024 12:02 | 04-01-2024 20:25 | 44.44340994 |
| CMS-7 | B | Dehydrator-1 | 05-01-2024 12:21 | 05-01-2024 14:09 | 26.4754512 |
| CMS-8 | B | Separator-2 | 05-01-2024 18:40 | 06-01-2024 15:03 | 10.2931667 |
| CMS-9 | B | Dehydrator-1 | 06-01-2024 12:55 | 07-01-2024 6:39 | 22.90488356 |
| CMS-10 | B | Separator-3 | 07-01-2024 3:28 | 07-01-2024 7:34 | 4.38235222 |
| CMS-11 | B | Tank-1 | 07-01-2024 15:50 | 08-01-2024 5:10 | 15.68792648 |
| CMS-12 | B | Dehydrator-1 | 08-01-2024 21:11 | 09-01-2024 5:36 | 23.01335768 |
| CMS-13 | B | Dehydrator-1 | 09-01-2024 4:54 | 09-01-2024 15:33 | 16.46214129 |
| CMS-14 | B | Dehydrator-1 | 09-01-2024 20:05 | 10-01-2024 10:21 | 6.575924082 |
| CMS-15 | B | Dehydrator-1 | 10-01-2024 9:17 | 11-01-2024 20:43 | 9.97428315 |
| CMS-16 | B | Tank-1 | 12-01-2024 8:57 | 15-01-2024 9:31 | 39.60280338 |
| CMS-17 | B | Dehydrator-1 | 15-01-2024 9:19 | 15-01-2024 12:30 | 4.631917288 |
| CMS-18 | B | Compressor-2 | 15-01-2024 11:46 | 16-01-2024 6:06 | 127.1398731 |
| CMS-19 | B | Compressor-3 | 16-01-2024 11:53 | 17-01-2024 3:15 | 50.81348771 |
| CMS-20 | B | Compressor-2 | 17-01-2024 10:29 | 19-01-2024 23:15 | 9.865365612 |
| CMS-21 | B | Tank-2 | 20-01-2024 17:49 | 21-01-2024 0:07 | 7.830741333 |
| CMS-22 | B | Compressor-2 | 21-01-2024 7:16 | 22-01-2024 0:02 | 7.280364451 |
| CMS-23 | B | Compressor-3 | 22-01-2024 2:24 | 22-01-2024 7:15 | 1.872333732 |
| CMS-24 | B | Wellhead | 22-01-2024 6:48 | 23-01-2024 1:56 | 11.11957246 |
| CMS-25 | B | Tank-1 | 22-01-2024 13:05 | 23-01-2024 2:59 | 15.78909064 |
| CMS-26 | B | Dehydrator-1 | 23-01-2024 16:02 | 24-01-2024 8:27 | 19.49150927 |
| CMS-27 | B | Compressor-1 | 23-01-2024 16:02 | 24-01-2024 6:27 | 27.31177958 |
| CMS-28 | B | Dehydrator-1 | 24-01-2024 15:06 | 25-01-2024 1:46 | 17.92923359 |
| CMS-29 | B | Separator-2 | 25-01-2024 16:45 | 26-01-2024 5:08 | 19.41097409 |
| CMS-30 | B | Dehydrator-1 | 26-01-2024 13:50 | 27-01-2024 6:36 | 22.35054016 |
| CMS-31 | B | Dehydrator-1 | 27-01-2024 1:45 | 27-01-2024 8:08 | 13.98306741 |
| CMS-32 | B | Separator-2 | 27-01-2024 10:10 | 28-01-2024 3:15 | 13.09969511 |
| CMS-33 | B | Compressor-1 | 27-01-2024 10:10 | 27-01-2024 23:37 | 16.04159662 |
| CMS-34 | B | Separator-2 | 28-01-2024 15:43 | 28-01-2024 23:59 | 10.05147194 |
| CMS-35 | B | Dehydrator-1 | 29-01-2024 15:48 | 30-01-2024 0:36 | 12.67874941 |
| CMS-36 | B | Tank-2 | 31-01-2024 17:15 | 01-02-2024 3:30 | 60.47970498 |

889

890

891

892

893 **References**

- 894 1. Allen, J. F. Maintaining Knowledge about Temporal Intervals. *Commun. ACM* **1983**, 26 (11),
895 832–843. <https://doi.org/10.1145/182.358434>.

896